

NASA TECHNICAL NOTE



NASA TN D-6546

c. 1

NASA TN D-6546

**LOAN COPY: RE
AFWL (DO
KIRTLAND AFI**



**VACUUM AND ULTRAVIOLET-RADIATION
EFFECTS ON BINDERS AND PIGMENTS FOR
SPACECRAFT THERMAL-CONTROL COATINGS**

by Donald J. Progar and William R. Wade

*Langley Research Center
Hampton, Va. 23365*

NATIONAL AERONAUTICS AND SPACE ADMINISTRATION • WASHINGTON, D. C. • NOVEMBER 1971

ERRATA

NASA Technical Note D-6546

VACUUM AND ULTRAVIOLET-RADIATION EFFECTS ON BINDERS AND
PIGMENTS FOR SPACECRAFT THERMAL-CONTROL COATINGS

By Donald J. Progar and William R. Wade
November 1971

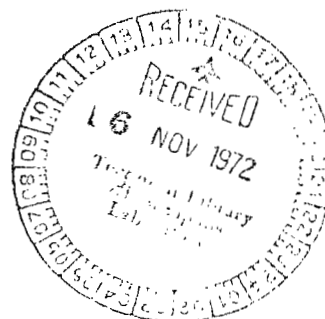
Page 15: The first term on the right-hand side of equation (8) should be -0.055 instead of -0.55.

Page 16: The first four lines should be reworded as follows:
(where x and y are Cartesian coordinates) or, in reflectance notation,
 $R'_{\lambda,S}$, the spectral reflectance of the sample corrected for the effect of the quartz tube, is

$$R'_{\lambda,S} = R_{\lambda,S} - 0.055 + 0.144R_{\lambda,S} - 0.050R_{\lambda,S}^2 \quad (9)$$

where $R_{\lambda,S}$ is the measured spectral reflectance of the sample. The values of

Issued October 1972



Errata inserted
7 Nov 72 Jh



0133391

1. Report No. NASA TN D-6546	2. Government Accession No.	3. Recipient's Catalog No.
4. Title and Subtitle VACUUM AND ULTRAVIOLET-RADIATION EFFECTS ON BINDERS AND PIGMENTS FOR SPACECRAFT THERMAL-CONTROL COATINGS		5. Report Date November 1971
7. Author(s) Donald J. Progar and William R. Wade		6. Performing Organization Code
9. Performing Organization Name and Address NASA Langley Research Center Hampton, Va. 23365		8. Performing Organization Report No. L-7722
12. Sponsoring Agency Name and Address National Aeronautics and Space Administration Washington, D.C. 20546		10. Work Unit No. 114-03-50-01
15. Supplementary Notes		11. Contract or Grant No.
16. Abstract <p>This paper presents an evaluation of several silicone resin binders and powdered inorganic pigments for potential use in spacecraft thermal-control paint formulations. The pigments were selected on the basis of a hypothesis relating the heat of formation of a compound to the compound's resistance to ultraviolet-radiation-induced degradation. Reflectance measurements were made in situ to determine degradation rates due to ultraviolet radiation. The tested polydimethylsiloxane resins were not significantly affected by long exposures to ultraviolet radiation. All the pigments, which were dispersed in a polydimethylsiloxane resin, were degraded by ultraviolet radiation as determined by an increase of solar absorptance. For the materials evaluated in this study, no evidence was found to indicate that pigments with high heats of formation were resistant to ultraviolet degradation.</p>		13. Type of Report and Period Covered Technical Note
17. Key Words (Suggested by Author(s)) Passive thermal control Radiation effects Solar ultraviolet radiation Silicones and pigments Vacuum effects Spacecraft coatings	18. Distribution Statement Unclassified - Unlimited	14. Sponsoring Agency Code
19. Security Classif. (of this report) Unclassified	20. Security Classif. (of this page) Unclassified	21. No. of Pages 42
		22. Price* \$3.00

VACUUM AND ULTRAVIOLET-RADIATION EFFECTS ON BINDERS AND PIGMENTS FOR SPACECRAFT THERMAL-CONTROL COATINGS

By Donald J. Progar and William R. Wade
Langley Research Center

SUMMARY

This program was concerned with the evaluation of several silicone resin binders and powdered inorganic pigments for potential use in spacecraft thermal-control paint formulations. The binders selected were those that could be cured without a catalyst, which has been shown in previous studies to be responsible for much of the ultraviolet-radiation-induced degradation. The pigments were selected on the basis of a hypothesis relating the heat of formation of a compound to the compound's resistance to ultraviolet-radiation-induced degradation. The tests to determine degradation rates were conducted in situ in a modular ultraviolet irradiation system, and reflectance measurements were obtained over a wavelength range from 0.25 μm to 2.65 μm by use of a dual-beam spectrophotometer equipped with an absolute-measurement-type integrating sphere. The tested polydimethylsiloxane resins were not significantly affected by long exposures to ultraviolet radiation. None of the tested pigments were found to be resistant to ultraviolet-radiation-induced degradation; all showed increases in solar absorptance. These increases ranged from 0.016 for zinc sulfide (ZnS) to 0.130 for boron nitride (BN(c)) after 100 equivalent solar hours (ESH) of simulated solar ultraviolet radiation and from 0.067 for ZnS to 0.221 for the BN(c) after 500 ESH of simulated solar ultraviolet radiation. For the materials evaluated in this study, no evidence was found to indicate that pigments with a high heat of formation were resistant to ultraviolet degradation.

INTRODUCTION

Thermal control of spacecraft is necessary to restrict the temperature excursions within limits imposed by the payload. Passive thermal control uses the thermal radiative properties of the exterior surface of the space vehicle to obtain an optimum operating temperature by achieving a balance between heat input and output. Since the primary external heat input is from solar radiation, the ratio of the solar absorptance (α_s) to thermal emittance (ϵ_T) of the exterior surfaces governs the equilibrium temperature of the spacecraft. During direct solar exposure, ratios (α_s/ϵ_T) of 0.20 or less are generally desired.

The desirable physical properties of a passive-thermal-control surface include ease of application to complex shapes, flexibility, adherence, and cleanability and repairability. Many pigmented paint coatings have these desirable properties.

The radiation characteristics of a passive-thermal-control surface must also remain unchanged when the surface is exposed to the space environment. Experience has shown, however, that most metal oxide paint pigments which are suitable for use as thermal-control coatings are severely degraded by exposure to high vacuum and to solar ultraviolet radiation. This degradation results in an increase of the solar absorptance of the coating and thus reduces its effectiveness as a passive-thermal-control surface.

One phase of this program was concerned with the evaluation of several commercially available, low-temperature-curing silicone resins for use as binders for thermal-control coatings.

This investigation was primarily concerned with the evaluation of several metal oxides as potential thermal-control paint pigments. Most of the pigments included in this study were those which have high heats of formation. These pigments were chosen to determine if a correlation exists between the energy required for decomposition of a molecule (the heat of formation) and the energy available in the ultraviolet region of the solar spectrum that may cause photochemical decomposition of the molecule.

SYMBOLS

B_{λ}	black-body monochromatic emissive power, $\frac{W/cm^2}{\mu m}$
c	velocity of light in vacuum, 3×10^{10} cm/sec
$d\lambda$	wavelength increment, μm
E_m	energy required for photochemical decomposition of a molecule of compound, J/molecule
E_p	energy of a discrete photon (that is, energy absorbed per molecule; see Einstein's photochemical equivalence law in appendix A), J
ΔH	heat of formation of one molecular weight of compound, J/mole
ΔH_m	heat of formation of one molecule of compound, J/molecule
h	Planck constant, 6.63×10^{-34} J-sec

J_{λ}	monochromatic radiation from a source (sun), $\frac{W/cm^2}{\mu m}$
N_A	Avogadro constant, 6.02×10^{23} molecules/mole
$R_{\lambda,s}$	measured spectral reflectance of sample
$R'_{\lambda,s}$	spectral reflectance of sample corrected for effect of quartz tube
$R_{\lambda,100}$	recorded 100-percent-reference spectral reflectance
$(R_{\lambda,s})_c$	corrected value of spectral reflectance of sample (corrected for 100-percent reference and effect of quartz tube)
t	elapsed time, min
V_O	baseline electromotive force (emf) generated by detector when optical path is closed, mV
V_R	emf generated by detector when platinum reference fin is viewed, mV
V_S	emf generated by detector when test sample is viewed, mV
α_S	solar absorptance
$\alpha_{S(1)}$	solar absorptance obtained in air in the quartz tube
$\alpha_{S(2)}$	solar absorptance obtained in vacuum in the quartz tube
$\alpha_{S(3)}$	solar absorptance obtained in vacuum in the quartz tube after periodic ultraviolet exposure
$\alpha_{S(4)}$	solar absorptance obtained immediately after admitting air into the system subsequent to ultraviolet exposure
$\Delta\alpha_S = \alpha_{S(3)} - \alpha_{S(2)}$	
ϵ_{TN}	total normal emittance of test sample at 300 K
λ	wavelength, cm or μm

ν	photon frequency, Hz
ρ_λ	monochromatic reflectance

ABBREVIATIONS

ESH	equivalent solar hours
PBR	pigment-binder ratio, by weight
UV	ultraviolet

PIGMENT SELECTION CRITERIA

The primary purpose of a thermal-control coating is to reflect as much of the incident solar energy as possible while radiating as much energy as possible, thereby preventing heat from reaching the interior of the spacecraft. The most important factors to consider in the reflectance of a thermal-control paint coating are (1) the particle size of the pigment, (2) the relative index of refraction of the pigment and binder, and (3) the weight of the pigment present in the coating (the pigment-binder ratio).

Maximum backscattering or reflectance is obtained when the particle size of the pigment is of the same order of magnitude as the wavelength of the incident radiation. All pigments included in this investigation had the highest purity with the smallest particle size distribution commercially available. Theoretically, for solar radiation a particle size of 2.5 μm or smaller is desirable. However, particle sizes used were for the most part larger than the size desired for maximum scattering. For greatest reflectance the index of refraction of the pigment should be significantly higher than that of the binder. Also a pigment-binder ratio that will give maximum backscatter should be used.

A further criterion for selection of many of the compounds was based on a hypothesis relating the standard heat of formation of the compound and the tendency of the pigment to undergo photochemical reactions when exposed to solar ultraviolet radiation in a high-vacuum environment. This hypothesis, originally proposed by William J. O'Sullivan, Jr., of Langley Research Center, can be stated thus: Photochemical decomposition of the pigment in a paint cannot occur unless the incident radiation contains photons of sufficient energy to cause the decomposition of the molecules of the compound into its separate elements or into a compound of lower molecular weight.

The rationale to determine a possible correlation between the degradation of the inorganic pigments studied in this program and their standard heat of formation is given in detail in appendix A.

BINDER SELECTION

It was originally believed that the silicone resins used as binder materials in thermal-control paints were not seriously affected by exposure to solar ultraviolet radiation. Investigations have shown, however, that many of the silicone resins considered stable are quite severely degraded by ultraviolet exposure (refs. 1 and 2). Photochemical reactions can occur because of additives, which are an important source of potential color-center formation within the polymer. These additives, which may be catalysts, solvents, stabilizers, or processing aids, must be considered with care if the introduction of ultraviolet absorbing impurities in the polymer is to be minimized (ref. 2).

The silicone resin binders included in this evaluation program are listed in table I. These resins do not require a catalyst to effect a complete cure, although a catalyst may be used to accelerate the cure. Thus, one source of potential color-center formation has been eliminated from the resins evaluated in this program. The resins were also selected as candidate binder materials on the basis of their desirable physical properties. All the resins are transparent to solar radiation, have adequate flexibility and strength, and are not damaged by moderate temperatures; in addition, most are resistant to thermal shock. These resins are also compatible with a wide variety of organic and inorganic materials.

TEST-SAMPLE PREPARATION

Silicone Resin Binders

Several commercially available silicone resins were selected for the evaluation of their stability in a space environment by the criteria discussed in the preceding section of this report. The silicone resin binders included in this investigation are listed in table II together with the solvents used and the cure schedule for each. Only one of the binders selected for this evaluation required a curing agent. This resin, RTV-615, was prepared for application by mixing one part of the manufacturer's curing agent to 10 parts of the resin.

The O-I Type 650 resin is received in a solid form and must be dissolved by the addition of a solvent, n-butanol, recommended by the manufacturer of the resin. The solvents shown in table II for the resins in the SR series were all added to the resins by the manufacturer, and the resins in the SR series were, therefore, used as received.

All known solvents used in the resins evaluated were of reagent grade and should have been volatilized during the resin cure schedule. Thus, no solvent residue should be present in the cured binder to act as potential color-center-formation sites during subsequent ultraviolet radiation.

Test samples were prepared by casting the silicone resin to inconel disks which had been polished with 240 through 600 grit emery paper and cleaned ultrasonically with petroleum ether and then acetone.

Pigmented Silicone Resins

In the phase of this program concerned with evaluation of the inorganic pigments, it was originally intended that the pigments would be tested in the form of compacted powders. This technique was unsuccessful because of the necessity of mounting test samples in a vertical position during ultraviolet radiation exposure and during measurement of the spectral reflectance of the test sample. The vertical placement resulted in the loss of surface particles during the test sequence, particularly during evacuation of the vacuum test chamber. Thus it was decided that the pigments should be combined with a silicone resin binder (O-I Type 650) which had been determined in this investigation to remain stable during long-term exposure to a simulated space environment of high vacuum and ultraviolet radiation.

Preparation of the pigmented-silicone-resin test samples consisted of combining the pigments with the selected binder resin in the pigment-binder ratios (PBR) shown in table III. The combination, which included the pigment and silicone resin in a solvent, was mixed in a conventional ball mill for approximately 1 hour. The pigmented silicone resin was then cast on ultrasonically cleaned inconel substrates polished with 240 through 600 grit emery paper. The test samples were then cured at the temperatures and for the time periods shown in table III.

In the preparation of these test samples, no attempt was made to reduce the particle size of the pigments or to further purify the pigments. It was considered that further size reduction could conceivably introduce additional lattice defects or impurities and thus contribute potential color-center-formation sites.

APPARATUS AND TEST PROCEDURES

The apparatus used in this program consisted of three main systems: the simulated space environment system, the in situ reflectance measurement system, and the room-temperature total-emittance measurement system. (In situ, in this paper, means that the test samples were maintained in a vacuum.) The reflectance and emittance measurement systems are equipped with automatic data readout in a form suitable for direct input to

machine computers for reduction of the raw data to values of thermal radiative properties. The details of these three systems are discussed separately.

Simulated Space Environment

The system used to expose test samples to a simulated space environment of high vacuum and ultraviolet radiation is shown in figure 1. In this system an ultraviolet source is located in a central housing which is equipped with an air blower for cooling a 1000-watt xenon arc lamp and an exhaust for removal of ozone produced by the ultraviolet radiation. The total radiation output of the lamp is continuously monitored by a photocell detector. Radiation from the xenon lamp is focused on the front surface of a test sample by a movable lens mounted in a covered optical path which extends radially from the lamp housing. In figure 1 the cover has been removed from the optical path to show this lens. The focusing lens can be moved to vary the intensity of radiation incident on the test samples from 0.5 to 5.0 equivalent ultraviolet suns. An ultraviolet sun is defined as the intensity of the solar ultraviolet radiation incident on a body 1 astronomical unit from the Sun. The intensity of the ultraviolet radiation incident on the test-sample face is determined by use of a filtered solar cell detector and a meter calibrated to read directly in equivalent ultraviolet suns. The wavelength ultimately reaching the test sample is determined by the transmission of the xenon-lamp envelope, which has a cutoff at about $0.19 \mu\text{m}$. During space stability evaluation, the test samples were mounted in individual stainless-steel vacuum chambers, each equipped with a 25-liter/sec ionization pump. One test-sample chamber, shown in figure 2, has a quartz window which transmits the simulated solar ultraviolet radiation to the test sample and also shows the quartz tube which permits in situ measurement of the spectral reflectance of the test sample. The test sample is mounted on a water-cooled support fixed to the end of a high-vacuum push-pull feedthrough, as shown in figure 2. This feedthrough is used to manipulate the test sample in the vacuum chamber; it allows movement of the sample from the ultraviolet-exposure position, directly behind the quartz window, to the reflectance position in the quartz tube. A thermocouple junction, attached to the water-cooled sample support, provides an indication of sample temperature, which did not change during the tests.

In Situ Reflectance Measurements

In situ spectral reflectance measurements are made by using the spectroreflectometer shown in figure 3. This spectroreflectometer is a dual-beam ratio-recording instrument equipped with an absolute-measurement-type integrating sphere. The sphere is constructed to allow center mounting of a test sample and provides absolute reflectance measurements (does not require a reference standard). For the reflectance measurements included in this report, the interior of the sphere was coated with an opaque coating of barium sulfate. This material has proven more durable than the conventional

magnesium oxide coating while still providing the diffuse, highly reflective wall coating required for these measurements. The spectroreflectometer is equipped with tungsten and xenon arc sources and with photomultiplier and lead sulfide detectors to allow efficient operation over the wavelength range from 0.25 μm to 2.65 μm .

When a spectral reflectance measurement was to be made in situ, the test-sample vacuum station was placed on the integrating sphere, as shown in figure 3, with the quartz tube projecting into the center of the sphere. The sample was moved into the quartz tube by use of the push-pull feedthrough, and the in situ reflectance measurement was performed.

The test-procedure sequence used during this program was as follows:

- (1) Determination of $(R_{\lambda,s})_c$ in air (through quartz tube of vacuum chamber)
- (2) Evacuation of the test-sample vacuum chamber to a pressure of 1.33×10^{-5} N/m² or less, followed by determination of $(R_{\lambda,s})_c$ in situ prior to ultraviolet irradiation (to determine effects of reduced pressure on test surface)
- (3) Beginning of solar ultraviolet irradiation of the test sample at an intensity of 3 equivalent ultraviolet suns, with periodic determination of $(R_{\lambda,s})_c$ in situ to determine the degradation of the test surface as a result of simulated solar ultraviolet radiation
- (4) Final determination of $(R_{\lambda,s})_c$ in air (through quartz tube) to establish bleaching effects.

Data Acquisition and Reduction

A technique for data acquisition and reduction was developed during this test program to convert measured values of spectral reflectance to values of solar absorptance. The technique uses an incremental digital tape system that was programed to initiate a data-point record sequence as a function of elapsed time. This recorder was used in conjunction with the linear-wavelength drive mechanism of the reflectometer, which allows the raw reflectance data to be referenced to the appropriate wavelength for the data recording and data reduction. The details of the data acquisition and reduction program are given in appendix B.

Room-Temperature Emittance Measurements

Although this investigation was intended primarily to provide information on the stability of the solar absorptance of white inorganic pigments when exposed to a simulated space environment, the values of total normal emittance for each test sample were also measured. The total-emittance values were obtained for each of the pigmented-silicone-resin coatings by use of equation (13).

The room-temperature emittance measurement apparatus shown in figure 4 consists of a heated-cavity reflectometer, a single-beam prism monochromator with a vacuum thermocouple detector, a linear amplifier, a strip-chart recorder, and a data readout system which records the raw data on punched cards for direct input to a computer.

In operation, a test sample is mounted on a water-cooled support and inserted into the cylindrical isothermal cavity where walls are maintained at an average temperature of 1033 K. Radiation from the cavity walls is reflected by the test sample (or a platinum reference fin) and transmitted by an optical transfer system to the single-beam monochromator. The reflected energy is then focused onto the thermocouple detector by the monochromator optics. The emf generated by the thermocouple detector is routed to the thermocouple amplifier and then to a strip-chart recorder. This recorder is equipped with a shaft digitizer where the signal is digitized for input to a summary card punch. The automated data readout system stores the sample reflectance value, the 100-percent reference value, and the zero (baseline) value; then a signal is given to transfer this information into punched cards along with various test constants and data programming information used in the calculation and tabulation of emittance data. The data reduction for calculation of the emittance is given in appendix B.

RESULTS AND DISCUSSION

Silicone Resin Binders

The results of the investigation to determine the resistance to optical degradation of the silicone resin binders exposed to a simulated space environment of high vacuum and ultraviolet radiation are shown in table IV.

The results for the SR series of resins show that all these silicone resins are degraded by 100 ESH of simulated solar ultraviolet radiation. The results obtained for the polyester-polymethylphenylsiloxane copolymers (SR-119 and SR-121) indicate less degradation after 500 ESH than that shown for the polymethylphenylsiloxanes (SR-82 and SR-112). However, all the resins in the SR series showed extensive degradation due to ultraviolet radiation and thus can be eliminated from further consideration as thermal-control paint binders.

The polydimethylsiloxane resins, RTV-615 and O-I Type 650, both show good resistance to ultraviolet-radiation-induced degradation. The test results for these materials show no significant degradation after more than 800 ESH of simulated solar ultraviolet radiation.

On the basis of these test results, either of the polydimethylsiloxane resins could be used as a binder for the powdered pigments subsequently evaluated. The selection of O-I Type 650 was made primarily because it is a one-component binder. The $\Delta\alpha_s$ of

0.008 shown in table IV was considered insignificant. The reflectance curves for the O-I Type 650 resin on a polished inconel substrate (fig. 5) show the effects of reduced pressure, ultraviolet radiation, and the re-exposure to air after in situ testing. The curves show no significant change in the spectral reflectance of this resin from the original reflectance measurement made in air prior to the simulated space exposures.

Pigment and Binder Coatings

The powdered pigments could not be effectively evaluated by themselves since the test samples were installed in a vertical position during ultraviolet exposure and measurement of reflectance. Therefore the pigments were combined with a silicone resin binder (O-I Type 650) previously determined to be resistant to high vacuum and ultraviolet radiation.

The tabulated results shown in table V include the initial values of solar absorptance prior to vacuum and ultraviolet exposure, the effect of reduced pressure on the solar absorptance, the effect of ultraviolet irradiation at an intensity of 3 equivalent ultraviolet suns, and the effect of air on the test surface immediately after ultraviolet irradiation was concluded. Figure 6 presents curves of spectral reflectance for the test samples over a wavelength range of 0.25 μm to 2.65 μm . These curves show the initial reflectance as well as changes in reflectance after reducing the pressure, after ultraviolet radiation in vacuum, and after subsequent exposure to air.

From figure 6 the effects of reduced pressure on the pigmented-silicone-resin test coatings are shown to be very similar for all coatings tested. In the infrared region of the spectrum from approximately 1.4 μm to 2.6 μm , the increase in the reflectance of the coatings due to reduced pressure is probably caused by the removal of water from the test sample by outgassing.

The results in table V and figure 6 showing the effects of ultraviolet exposure indicate that all the test coatings were severely degraded after only 100 ESH of simulated solar ultraviolet radiation with some samples showing increases in solar absorptance of more than 100 percent. The increases in the values of solar absorptance ranged from 0.016 for zinc sulfide (ZnS) to 0.130 for boron nitride (BN(c)) after 100 ESH of simulated solar ultraviolet radiation and from 0.067 for ZnS to 0.221 for BN(c) after 500 ESH of simulated solar ultraviolet radiation.

The experimental data obtained in this study did not verify the hypothesis intended to correlate the heat of formation of a compound with its resistance to ultraviolet-radiation-induced degradation. The tantalum pentoxide (Ta_2O_5) pigment compound, which has the highest heat of formation of the test materials (-2092 kJ/mole as shown in table VI), was severely degraded by ultraviolet radiation, with values of $\Delta\alpha_s$ of 0.106 and 0.120 (for the materials from two different vendors) after 500 ESH (see table V). However, this

material can be decomposed into lower molecular weight compounds. If the lanthanum trioxide (La_2O_3) with a heat of formation of -1916 kJ/mole is considered, the test results show even greater degradation, with values of $\Delta\alpha_s$ of 0.185 and 0.221 (for materials from two different vendors) after 500 ESH. The remaining test compounds having a heat of formation ΔH greater than the theoretical critical value of -996 kJ/mole (that is, hafnium dioxide (HfO_2), zirconium dioxide (ZrO_2), and gadolinium trioxide (Gd_2O_3)) all show high rates of degradation due to vacuum and ultraviolet irradiation. Conversely, those materials having low values of heat of formation (boron nitride with a heat of formation of -134 kJ/mole and zinc sulfide with a heat of formation of -201 kJ/mole) showed equal or less degradation than those compounds with high values of heat of formation. These results indicate that the ultraviolet-radiation-induced degradation of potential thermal-control coatings is strongly influenced by factors other than the standard heat of formation.

After ultraviolet exposures were completed, the effect of air on the ultraviolet degraded test surfaces was determined. All the test coatings, except Gd_2O_3 with O-I Type 650 resin, exhibited significant bleaching effects upon admission of air into the sample test chamber. In all cases, the result was an increase in the reflectance of the test coating and therefore is probably due to changes in the test-sample surface chemistry and not simply a reversal of the effects of reduced pressure. The reflectance curves in figure 6 show that the major bleaching of the test samples occurs in the range of the spectrum from $0.25 \mu\text{m}$ to $1.4 \mu\text{m}$, where the greatest ultraviolet degradation occurs.

CONCLUDING REMARKS

Of the silicone resins evaluated for their stability when exposed to intense solar ultraviolet radiation at low pressure, only the polydimethylsiloxanes (RTV-615 and O-I Type 650) showed resistance to degradation. The polyester-polymethylphenylsiloxane copolymers and the polymethylphenylsiloxanes were all severely degraded by 100 equivalent solar hours (ESH) of simulated solar ultraviolet radiation.

The inorganic pigment materials which were dispersed in O-I Type 650 binder and evaluated in this study showed extensive degradation as a result of 100 ESH of simulated solar ultraviolet radiation. All showed increases in solar absorptance. These increases ranged from 0.016 for zinc sulfide (ZnS) to 0.130 for boron nitride (BN(c)) after 100 ESH of simulated solar ultraviolet radiation and from 0.067 for ZnS to 0.221 for the BN(c) after 500 ESH of simulated solar ultraviolet radiation.

No relationship between the heat of formation and resistance to ultraviolet-radiation-induced degradation of the pigments included in this study was indicated by the results of this evaluation.

Langley Research Center,
National Aeronautics and Space Administration,
Hampton, Va., October 22, 1971.

APPENDIX A

HYPOTHESIS: RELATION OF HEAT OF FORMATION TO ULTRAVIOLET DEGRADATION OF INORGANIC COMPOUNDS

The energy required for the photochemical decomposition of a molecule of paint-pigment compound is defined as E_m , and energy available in a discrete photon is defined as E_p . The postulated hypothesis is expressed mathematically as

$$E_p \cong E_m \quad (1)$$

If this hypothesis is to be used as a criterion for the selection of compounds for thermal-control paint pigments, it is necessary to determine these quantities, E_p and E_m . When a pigment compound is exposed to ultraviolet radiation, an incident photon may be either reflected or absorbed by a molecule of the compound, and the laws of photochemistry state (ref. 3) that (1) only the light which is absorbed can act chemically (Grothuss-Draper) and (2) each absorbed quantum should cause one light-absorbing molecule to react (Einstein's photochemical equivalence). These laws infer that a definite amount of energy is required to cause a photochemical reaction in a molecule and that this energy must be contained in one photon, not the summation of energies in two or more photons.

The energy distribution of the sun (ref. 4) as shown in figure 7 contains virtually no radiation below $0.12 \mu\text{m}$. The intensity is decreased by about five orders of magnitude from the peak intensity at near $0.5 \mu\text{m}$. Thus, it is reasonable to assume that the degradation of a paint pigment must be due to radiation of a wavelength higher than $0.12 \mu\text{m}$. If the wavelength of $0.12 \mu\text{m}$ is accepted as the critical wavelength, the energy content of a discrete photon at this wavelength can be calculated from

$$E_p = h\nu \quad (2)$$

Since $\nu = \frac{c}{\lambda}$,

$$E_p = \frac{hc}{\lambda} \quad (3)$$

where

E_p energy of the photon, joules

h Planck constant, 6.63×10^{-34} J-sec

c velocity of light in vacuum, 3×10^{10} cm/sec

λ wavelength of the photon, cm

APPENDIX A – Concluded

Equation (3) is solved as follows for the energy of a discrete photon of wavelength 0.12 μm :

$$E_p = \frac{(6.63 \times 10^{-34})(3 \times 10^{10})}{1.20 \times 10^{-5}} = 1.655 \times 10^{-18} \text{ joule} \quad (4)$$

One means of expressing the quantity E_m is in terms of the standard heat of formation ΔH which is a measure of the energy, expressed as heat, that is absorbed or released during the formation or decomposition of one molecular weight of a stable compound. From the standard heat of formation, the energy that is released in the formation of one molecule can be determined by the relation

$$\Delta H_m = \frac{\Delta H}{N_A} \quad (5)$$

where

ΔH heat of formation of one molecular weight of compound, J/mole

ΔH_m heat of formation of one molecule of compound, J/molecule

N_A Avogadro constant, 6.02×10^{23} molecules/mole

By definition $\Delta H_m = E_m$; thus equations (4) and (5) are used, with appropriate conversion factors, to set up the equation

$$E_p \cong E_m = \frac{\Delta H}{N_A} \quad (6)$$

and obtain $\Delta H \cong -996 \text{ kJ/mole}$ as the heat of formation that a compound must possess in order to be incapable of being decomposed photochemically by solar radiation of all wavelengths down to the critical wavelength of 0.12 μm . Care must be used in applying this criterion, however, since many compounds can be decomposed into compounds of lower molecular weight in which event their partial decomposition requires less energy than their ΔH as listed in various sources. Such cases can be identified by a study of the tables of compounds formed by the elements involved. The compounds selected by this criterion for evaluation in this program are listed in table VI with their ΔH , index of refraction, and any lower molecular weight compounds, as obtained from references 5 to 11.

APPENDIX B

DATA ACQUISITION AND REDUCTION

Solar Absorptance Measurements

The technique for data acquisition uses an incremental digital tape system which can be programed to initiate a data-point record sequence as a function of elapsed time. The recorder is used in conjunction with the variable-speed linear-wavelength drive mechanism of the reflectometer, which allows the raw reflectance data to be referenced to the appropriate wavelength in the data recording and subsequent data reduction.

A simplified schematic diagram of the data readout system is shown in figure 8. The strip-chart recorder, supplied with the reflectometer to provide a reflectance curve during the measurement, was modified by the installation of a retransmitting slidewire as shown in figure 8. The retransmitting slidewire is supplied with a 100-mV dc full-scale voltage by a constant voltage unit. The wiper of this slidewire is driven by the reflectometer recorder servomotor; thus displacement of the retransmitting slidewire wiper corresponds to the displacement of the recorder pen which indicates the value of measured spectral reflectance of the sample. The potential thus obtained by displacement of the retransmitting slidewire wiper is used as the input signal to the magnetic tape recorder.

In operation the magnetic tape recorder system is programed to initiate a record sequence each 0.1 minute, and the reflectometer wavelength drive is set to advance at the rate of 0.150 $\mu\text{m}/\text{min}$. Thus a reflectance data point is recorded for each 0.015 μm over the wavelength range of interest (from 0.25 μm to 2.65 μm). The data-reduction program was designed to convert the recorded values of elapsed time to the corresponding wavelength by the equation

$$\lambda = 0.235 \mu\text{m} + (0.150 \mu\text{m}/\text{min})t \quad (7)$$

where λ is the wavelength of the measured reflectance values in μm , 0.235 μm is the wavelength at $t = 0$, 0.150 $\mu\text{m}/\text{min}$ is the wavelength drive speed, and t is the elapsed time in minutes.

Spectral reflectance measurements are made in situ with the test sample mounted inside a Suprasil quartz tube. This procedure results in an error in the measured values of reflectance; this error is a function of the sample reflected energy. To obtain a correction factor for the in situ measurements, values of spectral reflectance ranging from 0.070 to 0.990 were obtained with the sample mounted both inside and outside the quartz tube. The values of experimental error were then fit to a curve determined by the method of least squares to have an equation

$$y = -0.55 + 0.144x - 0.05x^2 \quad (8)$$

APPENDIX B - Continued

(where x and y are Cartesian coordinates) or, in reflectance notation, $R'_{\lambda,s}$, the spectral reflectance of the sample corrected for the effect of the quartz tube, is

$$R'_{\lambda,s} = R_{\lambda,s} - 0.055 + 0.144R_{\lambda,s} - 0.050R_{\lambda,s}^2 \quad (9)$$

where $R_{\lambda,s}$ is the measured spectral reflectance of the sample. The values of $R'_{\lambda,s}$ were then divided by the 100-percent-reference value to obtain values of $(R_{\lambda,s})_c$. That is,

$$(R_{\lambda,s})_c = \frac{R'_{\lambda,s}}{R_{\lambda,100}} \quad (10)$$

Values of solar absorptance were then computed by the equation

$$\alpha_s = 1.00 - \frac{\int_{0.25 \mu\text{m}}^{2.65 \mu\text{m}} (R_{\lambda,s})_c J_\lambda d\lambda}{\int_{0.25 \mu\text{m}}^{2.65 \mu\text{m}} J_\lambda d\lambda} \quad (11)$$

where

α_s solar absorptance of sample

$(R_{\lambda,s})_c$ corrected value of spectral reflectance of sample (corrected for 100-percent reference and effect of quartz tube)

J_λ monochromatic radiation from a source (sun), $\frac{W/cm^2}{\mu\text{m}}$

$d\lambda$ wavelength increment, μm

Room-Temperature Total Normal Emittance

The data-reduction program calculates the monochromatic reflectance of the test sample by use of the relation

$$\rho_\lambda = \frac{V_s - V_o}{V_R - V_o} \quad (12)$$

where

V_s emf generated by thermocouple detector when test sample is being viewed, mV

V_R emf generated by detector when platinum reference fin is being viewed, mV

APPENDIX B – Concluded

V_o baseline emf generated by detector when optical path is closed (equivalent to noise or stray-light emf), mV

ρ_λ monochromatic reflectance

Total normal-emittance values are then determined by using the expression

$$\epsilon_{TN} = 1.0 - \frac{\int_{1 \mu m}^{25 \mu m} \rho_\lambda B_\lambda d\lambda}{\int_{1 \mu m}^{25 \mu m} B_\lambda d\lambda} \quad (13)$$

where

ϵ_{TN} total normal emittance of test sample at 300 K

B_λ monochromatic emissive power of a 300 K black body, $\frac{W/cm^2}{\mu m}$

$d\lambda$ wavelength interval (0.5 μm in this emittance program)

REFERENCES

1. Slemp, Wayne S.; and Hankinson, T. W. E.: Environmental Studies of Thermal Control Coatings for Lunar Orbiter. Thermal Design Principles of Spacecraft and Entry Bodies, Jerry T. Bevans, ed., Academic Press, Inc., 1969, pp. 797-817.
2. Caldwell, C. R.; and Nelson, P. A.: Thermal Control Experiments on the Lunar Orbiter Spacecraft. Thermal Design Principles of Spacecraft and Entry Bodies, Jerry T. Bevans, ed., Academic Press, Inc., 1969, pp. 819-852.
3. Lange, Norbert Adolph, compiler: Handbook of Chemistry. Sixth ed., Handbook, Publ., Inc., 1946, pp. 1643-1644.
4. Malitson, Harriet H.: The Solar Spectrum. Sky Telescope, vol. XXIX, no. 3, Mar. 1965, pp. 162-165.
5. Weast, Robert C.; Selby, Samuel M.; and Hodgman, Charles D., eds.: Handbook of Chemistry and Physics. Forty-fifth ed., Chem. Rubber Pub. Co., c.1964.
6. Coughlin, James P.: Contributions to the Data on Theoretical Metallurgy - XII. Heats and Free Energies of Formation of Inorganic Oxides. Bull. 542, Bur. Mines, U.S. Dept. Interior, 1954.
7. Sviridova, A. A.; and Suikovskaya, N. V.: Transparence Limits of Interference Films of Hafnium and Thorium Oxides in the Ultraviolet Region of the Spectrum. Opt. Spectry. (USSR), vol. XXII, no. 6, June 1967, pp. 509-512.
8. Hass, G.; Ramsey, J. B.; and Thun, R.: Optical Properties of Various Evaporated Rare Earth Oxides and Fluorides. J. Opt. Soc. Amer., vol. 49, no. 2, Feb. 1959, pp. 116-120.
9. Kumagai, S.; and Young, L.: Ellipsometric Investigation of the Optical Properties of Anodic Oxide Films on Tantalum. J. Electrochem. Soc., vol. 111, no. 12, Dec. 1964, pp. 1411-1416.
10. Wentorf, R. H., Jr.: Preparation of Semiconducting Cubic Boron Nitride. J. Chem. Phys., vol. 36, no. 8, Apr. 15, 1962, pp. 1990-1991.
11. Rideout, V. L.; and Wemple, S. H.: Optical Constants of Evaporated Gold and Platinum Films on Potassium Tantalate. J. Opt. Soc. Amer., vol. 56, no. 6, June 1966, pp. 749-751.

TABLE I.- CANDIDATE BINDER MATERIALS

Resin	Polymer
SR-82	Polymethylphenylsiloxane
SR-112	Polymethylphenylsiloxane
SR-119	Polyester-polymethylphenylsiloxane copolymer
SR-121	Polyester-polymethylphenylsiloxane copolymer
SR-125	Polymethylphenylsiloxane
RTV-615	Polydimethylsiloxane ^a
O-I Type 650	Polydimethylsiloxane

^a Requires curing agent.

TABLE II.- PREPARATION OF BINDER TEST SAMPLES

Resin	Solvents	Cure schedule	
		Temperature, K	Time, hr
SR-82	Xylol	522	1.5
SR-112	Xylol	522	1.5
SR-119	70% xylol; 30% n-butanol	449	1.0
SR-121	70% xylol; 30% n-butanol	491	.5
SR-125	Xylol	522	1.0
RTV-615		338	4.0
O-I Type 650	n-butanol	408	18.0

TABLE III.- PREPARATION OF PIGMENT AND O-I TYPE 650 COATINGS

Pigment compound (*)	Purity, percent	Particle size, μm	PBR	Coating thickness, μm	Cure schedule	
					Temperature, K	Time, hr
Gd ₂ O ₃	99.999	<74	8.3	210	408	18
HfO ₂	99.95	<74	8.3	550	408	18
La ₂ O ₃ (a)	99.999	0.15 to 1.0	4.1	660	373	18
La ₂ O ₃ (b)	99.99		3.3	970	408	18
Ta ₂ O ₅ (a)	99.95	5.0	6.6	780	408	18
Ta ₂ O ₅ (b)	99.95		5.5	580	408	18
ZrO ₂ (a)	99.5		5.3	670	408	18
ZrO ₂ (b)	99.99	1.0	1.9	400	403	18
BN(a)	99.9	10	.4	380	408	20
BN(b)	99.5	15	1.2	440	408	20
BN(c)	99.5	<44	1.1	460	408	18
KTaO ₃	99.9	<74	8.3	460	408	18
ZnS	99.95	<74	8.3	670	408	18

* The lower-case letters in parentheses after the compounds indicate different suppliers or different grades of the same compound from the same supplier.

TABLE IV.- RESULTS OF BINDER DEGRADATION TESTS

Binder material	Coating thickness, μm	$\alpha_{s(1)}$	$\alpha_{s(2)}$	Ultraviolet exposure, ESH	$\Delta\alpha_s$
SR-82	99	0.526	0.522	100	0.060
				500	.082
SR-112	101	.515	.515	100	.061
				500	.084
SR-119	53	.494	.496	100	.053
				500	.067
SR-121	76	.515	.515	100	.054
				500	.066
SR-125	155	.528	.525	100	.044
				500	.075
RTV-615	716	.508	.504	100	.001
				500	.003
				800	.005
O-I Type 650	25	.436	.430	100	.001
				500	.005
				800	.008

TABLE V.- EFFECTS OF HIGH VACUUM AND ULTRAVIOLET RADIATION ON SOLAR ABSORPTANCE
OF PIGMENTS COMBINED WITH O-I TYPE 650 RESIN

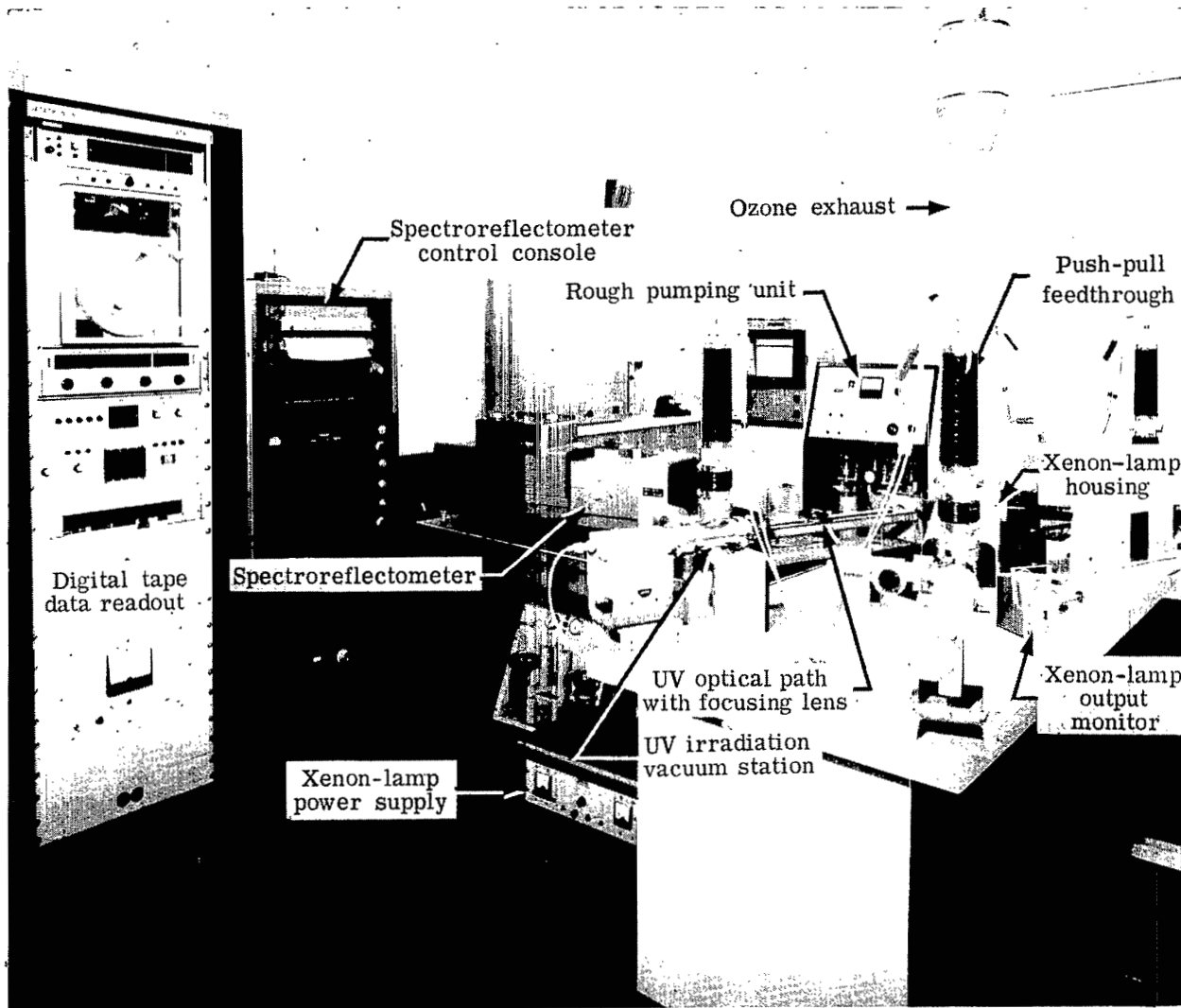
Pigment compound (*)	ϵ_{TN}	$\alpha_{s(1)}$	$\alpha_{s(2)}$	$\alpha_{s(2)} - \alpha_{s(1)}$	Ultraviolet exposure			$\alpha_{s(4)}$	$\alpha_{s(4)} - \alpha_{s(3)}$
					ESH	$\alpha_{s(3)}$	$\Delta\alpha_s$		
Gd ₂ O ₃	0.91	0.062	0.062	0	100	0.094	0.032	0.162	-0.009
					300	.135	.073		
					500	.171	.109		
HfO ₂	.82	.083	.090	.007	100	.163	.073	.271	-.038
					300	.253	.163		
					500	.298	.208		
					570	.309	.219		
La ₂ O ₃ (a)	.87	.088	.062	-.026	100	.146	.084	.233	-.014
					300	.212	.150		
					500	.247	.185		
La ₂ O ₃ (b)	.75	.097	.062	-.035	100	.157	.095	.259	-.024
					300	.232	.170		
					500	.283	.221		
Ta ₂ O ₅ (a)	.77	.089	.093	.004	100	.191	.098	.184	-.019
					300	.195	.102		
					500	.199	.106		
					760	.203	.110		
Ta ₂ O ₅ (b)	.82	.100	.105	.005	100	.217	.112	.191	-.040
					300	.221	.116		
					500	.225	.120		
					770	.231	.126		
ZrO ₂ (a)	.82	.057	.063	.006	100	.133	.070	.184	-.038
					300	.183	.120		
					500	.213	.150		
					550	.222	.159		
ZrO ₂ (b)	.88	.236	.240	.004	100	.345	.105	.470	-.012
					300	.421	.181		
					500	.458	.218		
					660	.482	.242		
BN(a)	.96	.397	.387	-.010	100	.419	.032	.469	-.021
					300	.450	.063		
					500	.481	.094		
					550	.490	.103		
BN(b)	.88	.121	.117	-.004	100	.163	.046	.204	-.019
					300	.193	.076		
					490	.223	.106		
BN(c)	.90	.261	.250	-.011	100	.280	.130	.458	-.013
					300	.431	.181		
					500	.471	.221		
KTaO ₃	.89	.096	.100	.004	100	.164	.064	.173	-.083
					300	.199	.099		
					500	.234	.134		
					625	.256	.156		
ZnS	.84	.110	.110	0	100	.126	.016	.154	-.025
					300	.158	.048		
					500	.177	.067		
					570	.179	.069		

*The lower-case letters in parentheses after the compounds indicate different suppliers or different grades of the same compound from the same supplier.

TABLE VI.- CANDIDATE PIGMENT MATERIALS

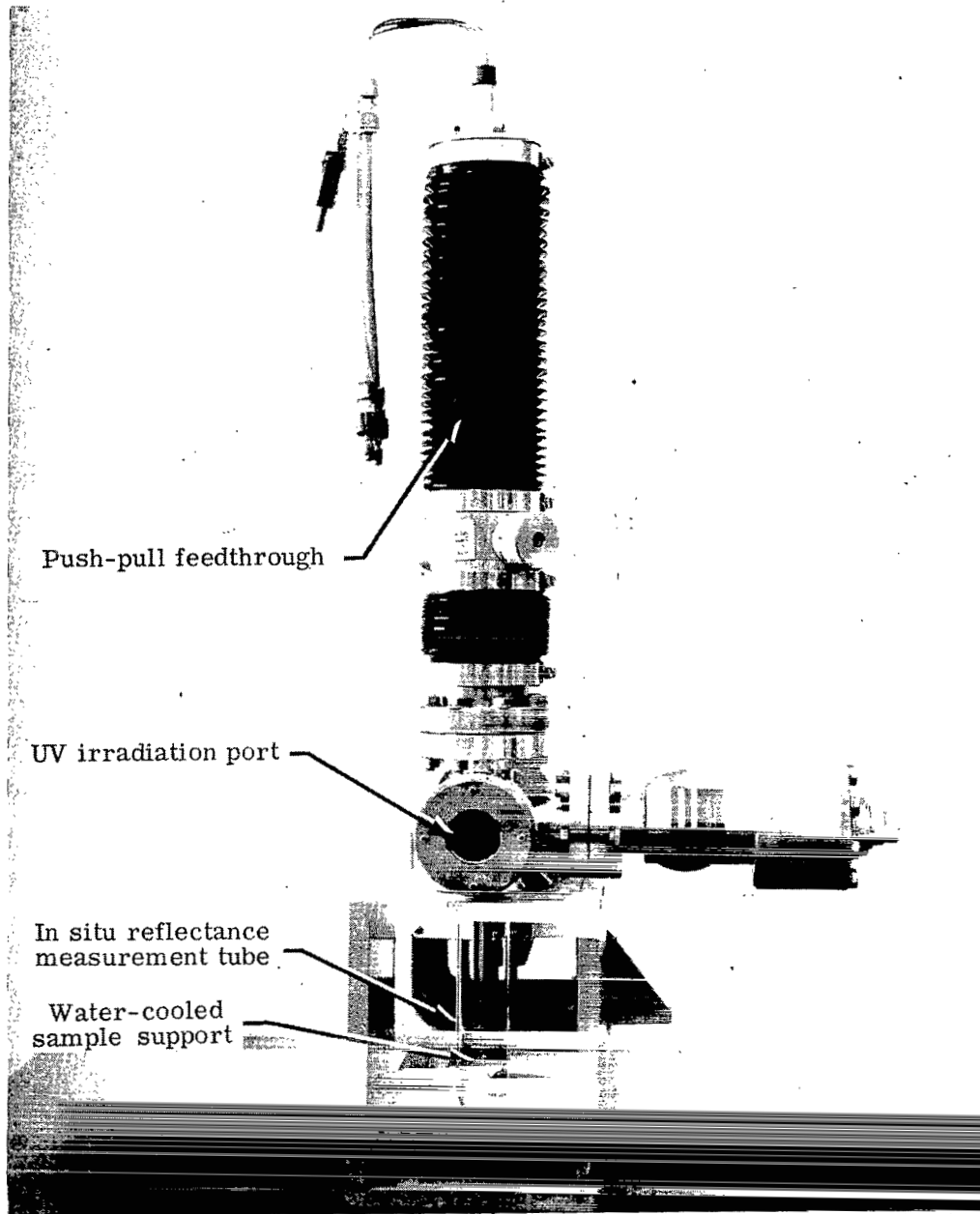
Pigment compound	Standard heat of formation, ΔH , kJ/mole (*)	Index of refraction	Lower molecular weight compounds
Ta ₂ O ₅	-2092	2.21 to 2.26	Ta ₂ O ₄ (or TaO ₂)
La ₂ O ₃	-1916	1.85 to 1.95	None
HfO ₂	-1134	2.05 to 2.06	None
Gd ₂ O ₃	-1079	2.05 to 2.20	Gd ₂ O
ZrO ₂	-1079	2.13 to 2.20	None
ZnS	-201	2.36 to 2.38	None
BN	-134	2.22	None
KTaO ₃	Not available	2.21 to 2.40	None

* The critical value of ΔH is -996 kJ/mole.



L-71-7111

Figure 1.- Overall view of UV irradiation apparatus and in situ reflectance measurement system.



L-71-7112

Figure 2.- Test-sample vacuum station.

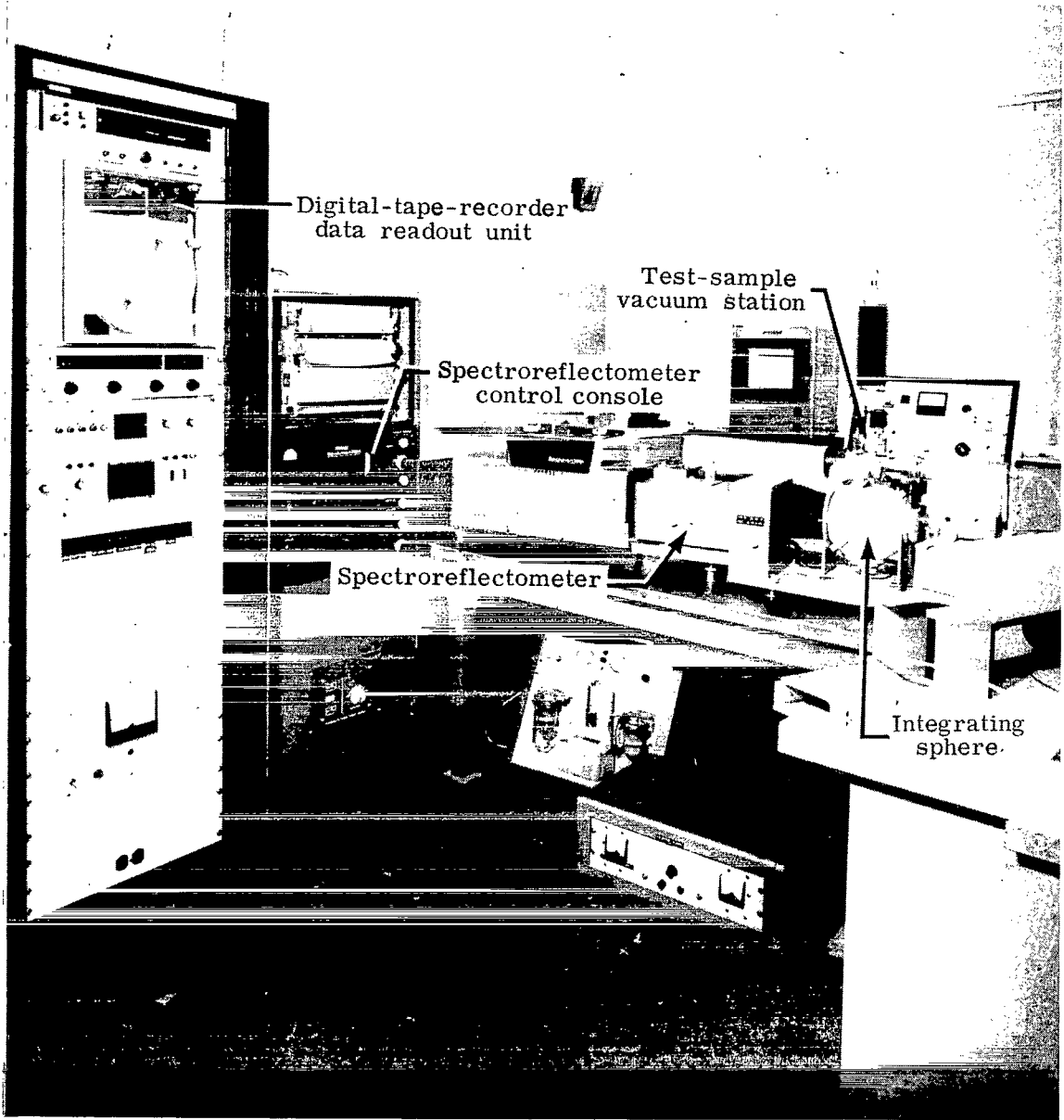


Figure 3.- In situ reflectance measurement system.

L-71-7113

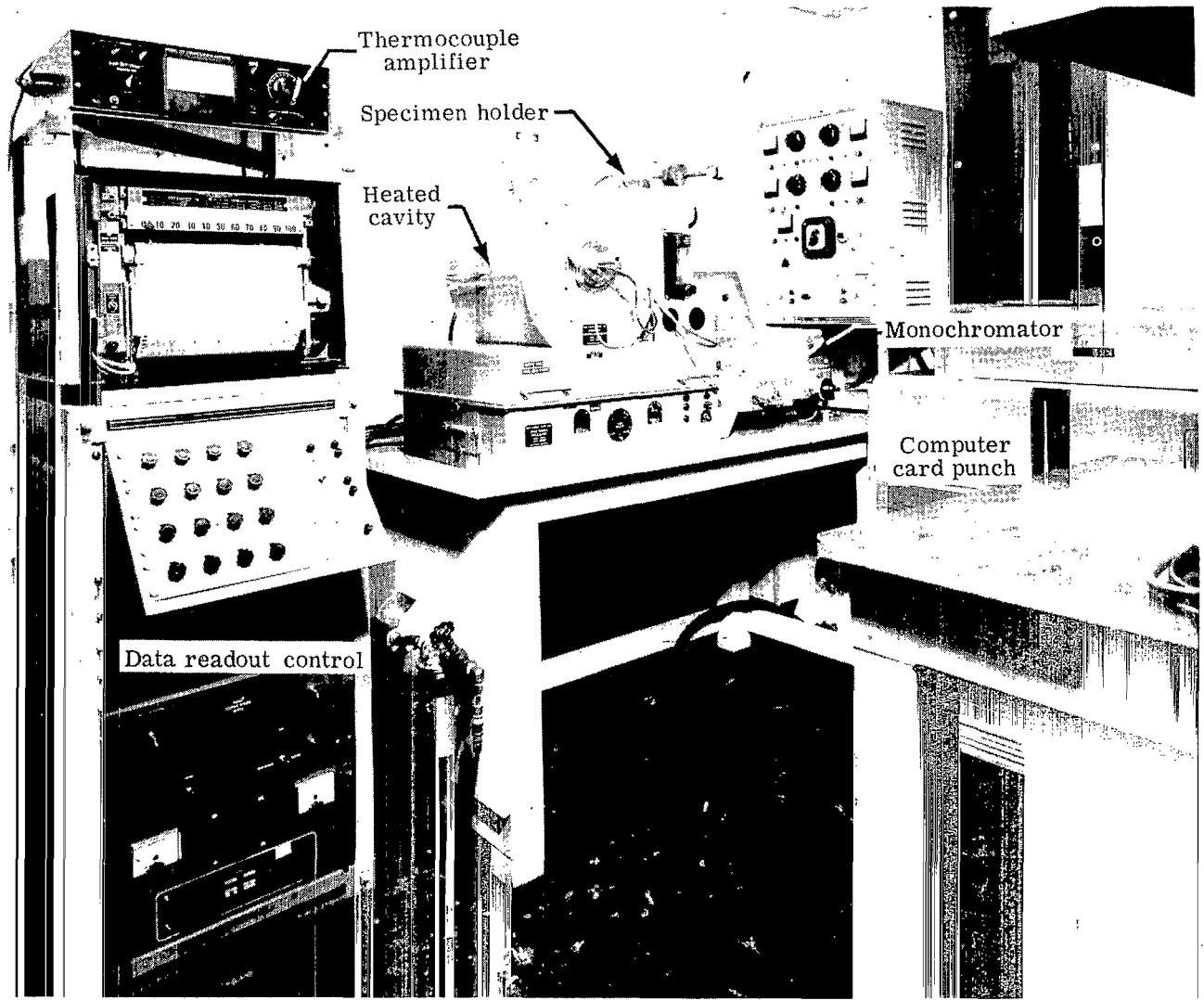


Figure 4.- Room-temperature emittance measurement apparatus.

L-71-7114

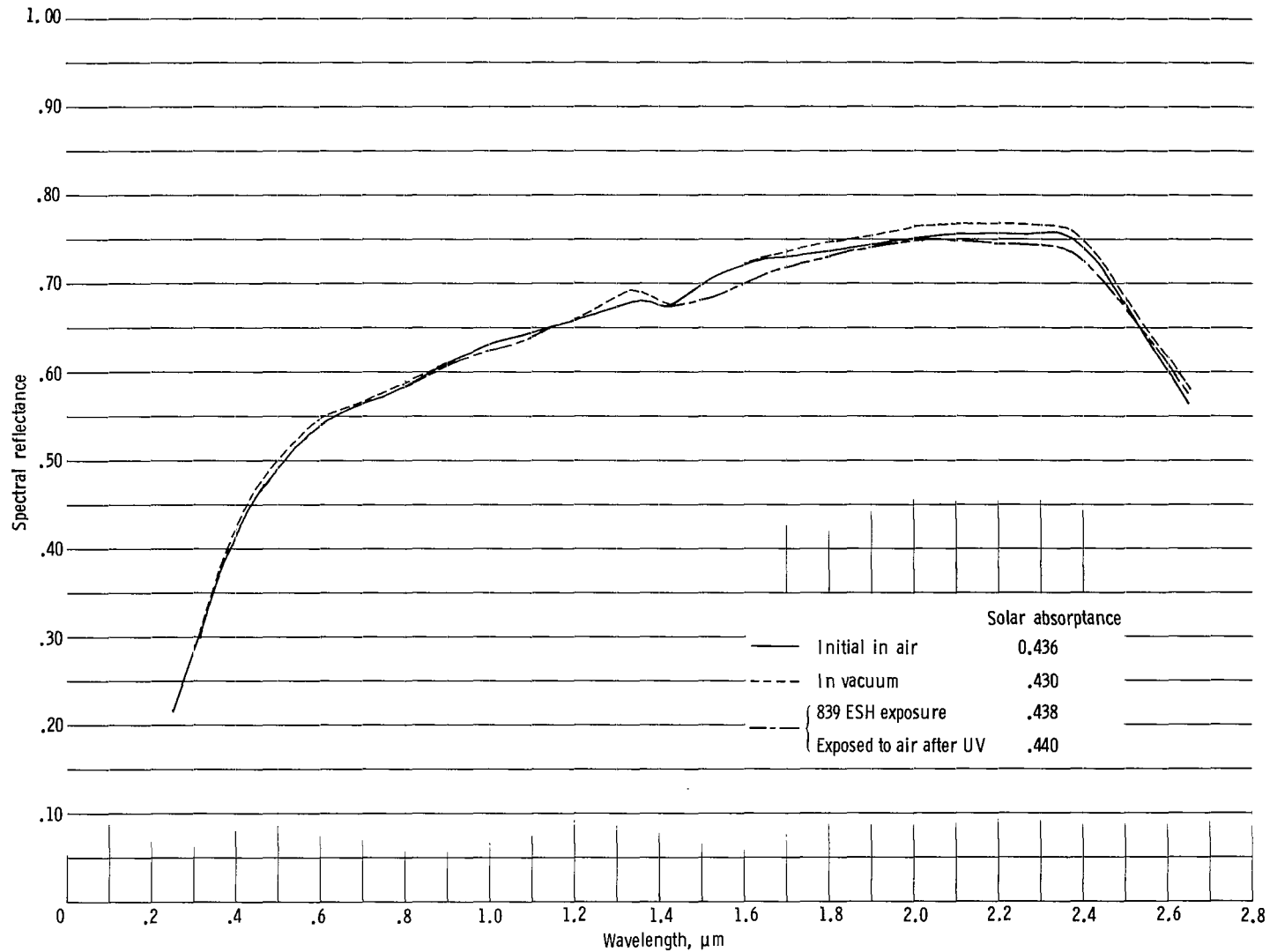
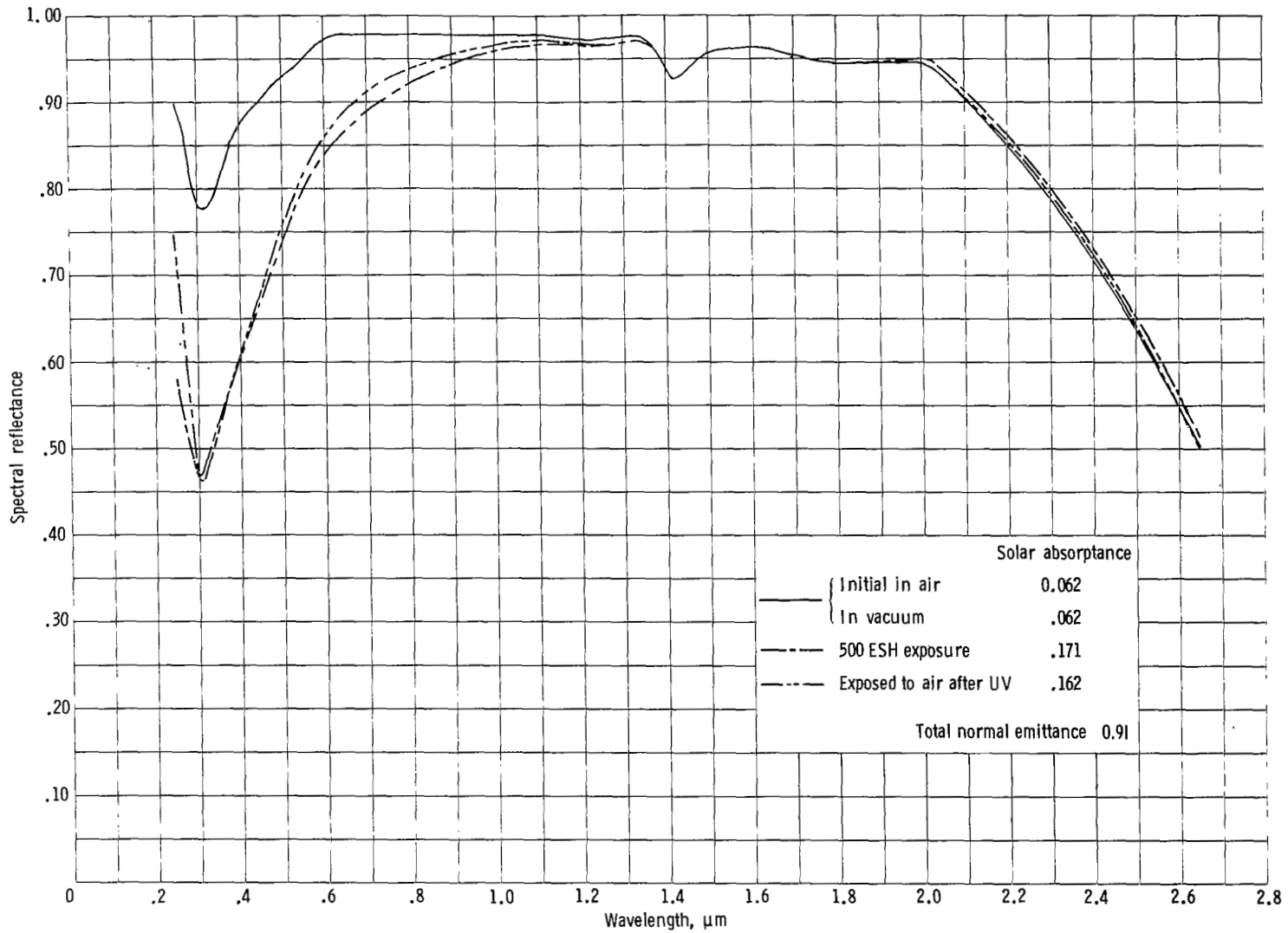
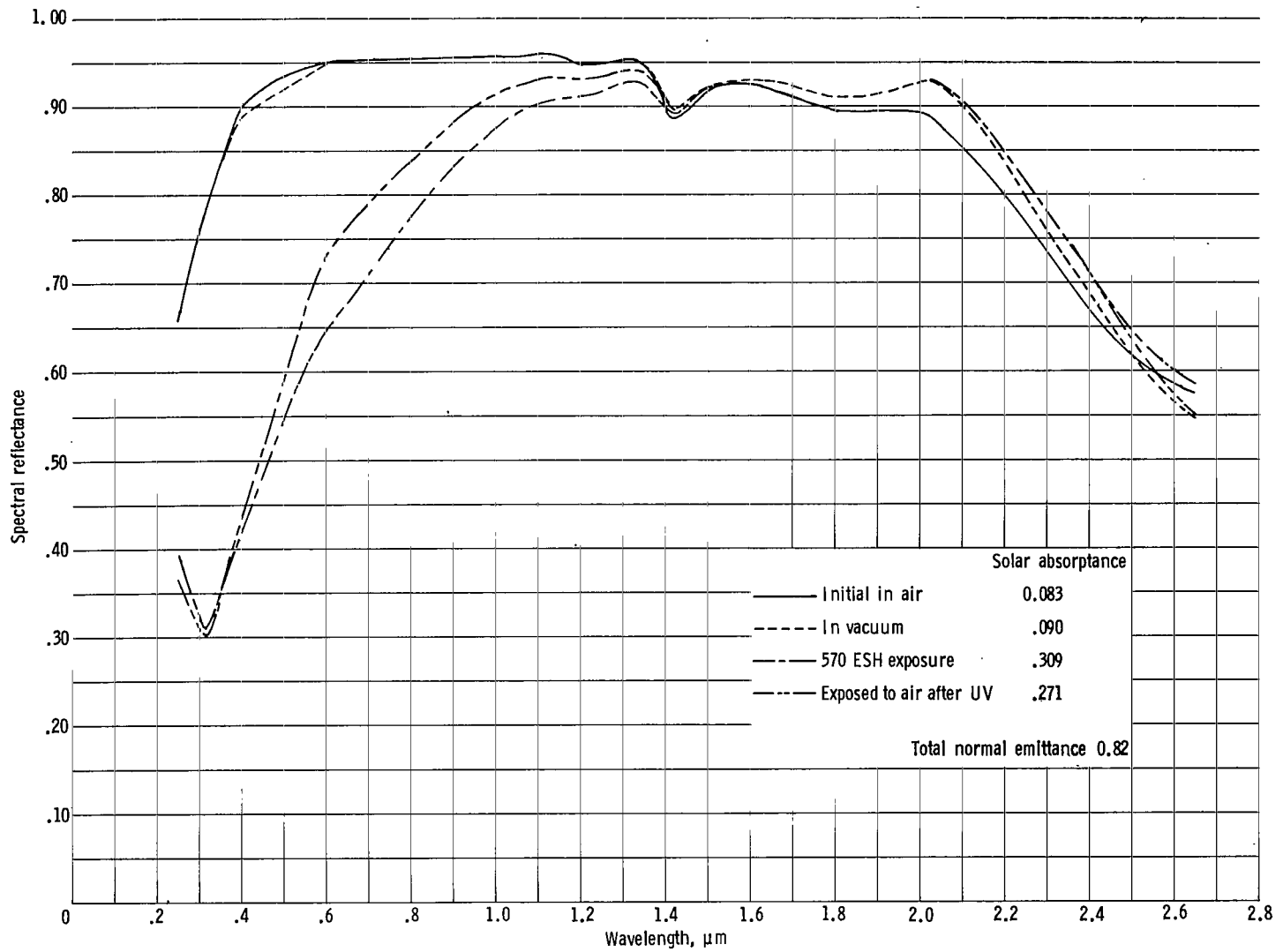


Figure 5.- Effects of vacuum and UV radiation on O-I Type 650 resin as determined by the variation of spectral reflectance $(R_{\lambda,S})_c$ with wavelength.



(a) Gd₂O₃ with O-I Type 650 resin.

Figure 6.- Effects of vacuum and UV radiation on test compounds as determined by the variation of spectral reflectance $(R_{\lambda,s})_c$ with wavelength.



(b) HfO_2 with O-I Type 650 resin.

Figure 6.- Continued.

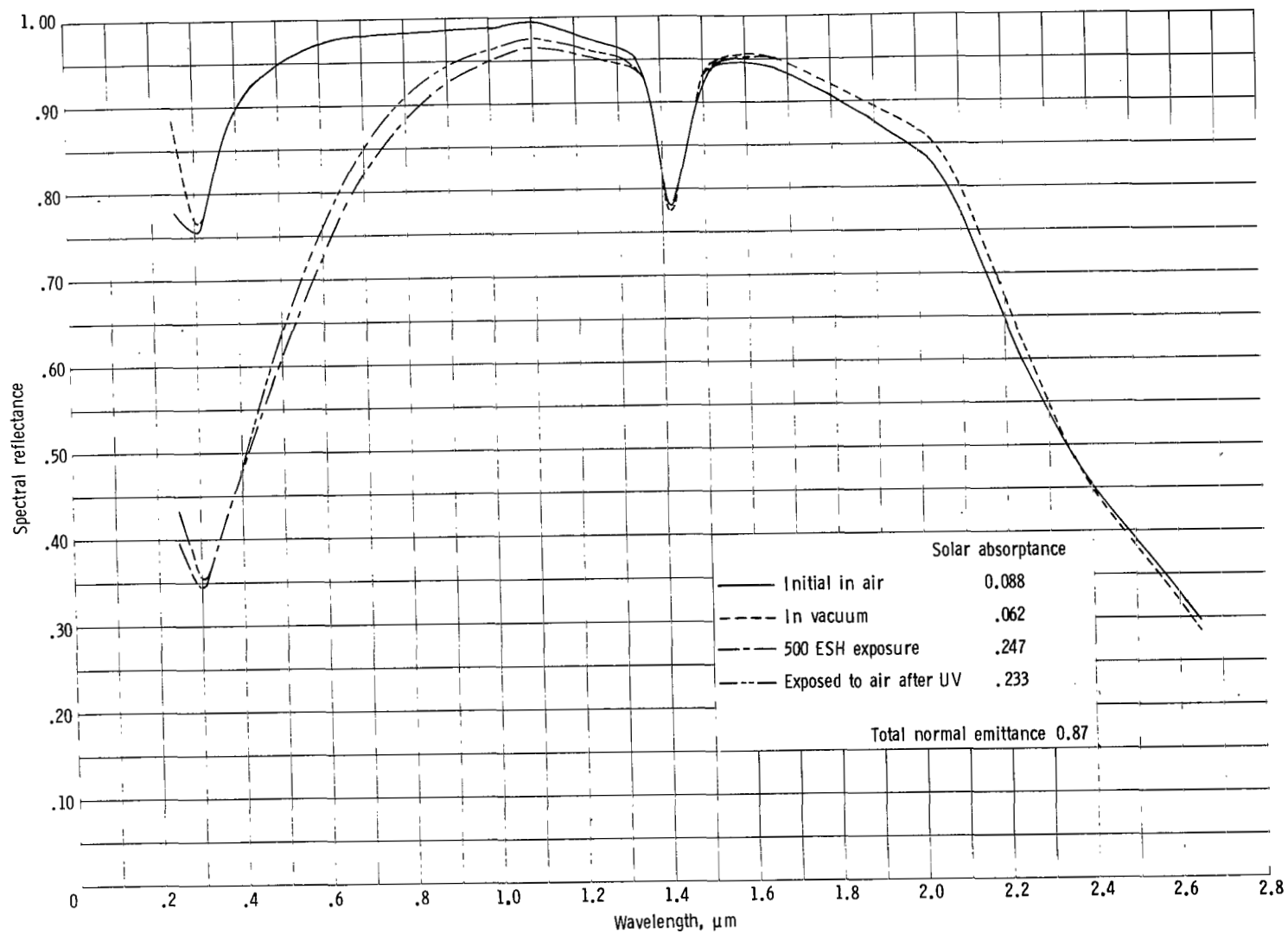
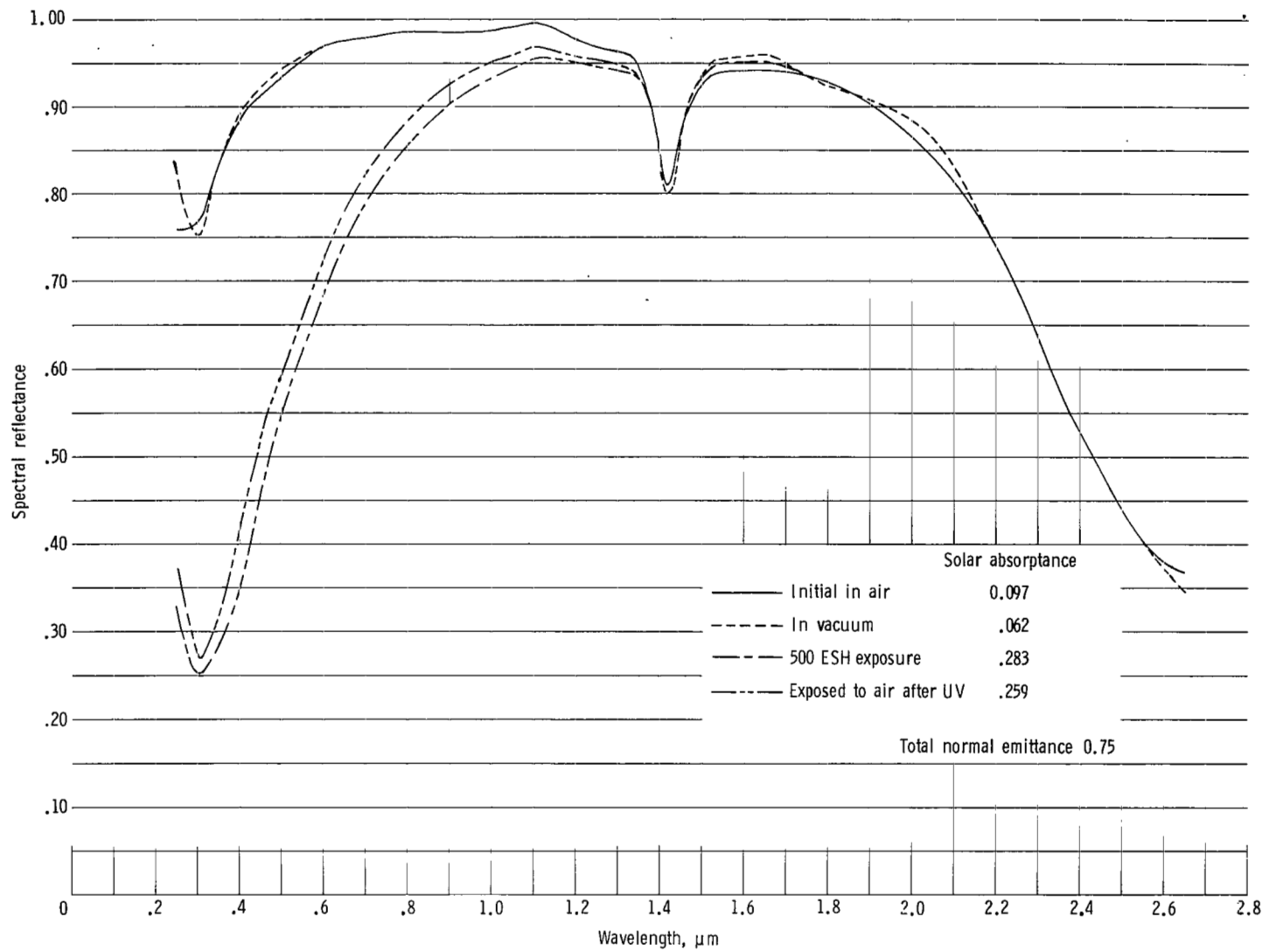
(c) $\text{La}_2\text{O}_3(\text{a})$ with O-I Type 650 resin.

Figure 6.- Continued.



(d) $\text{La}_2\text{O}_3(\text{b})$ with O-I Type 650 resin.

Figure 6.- Continued.

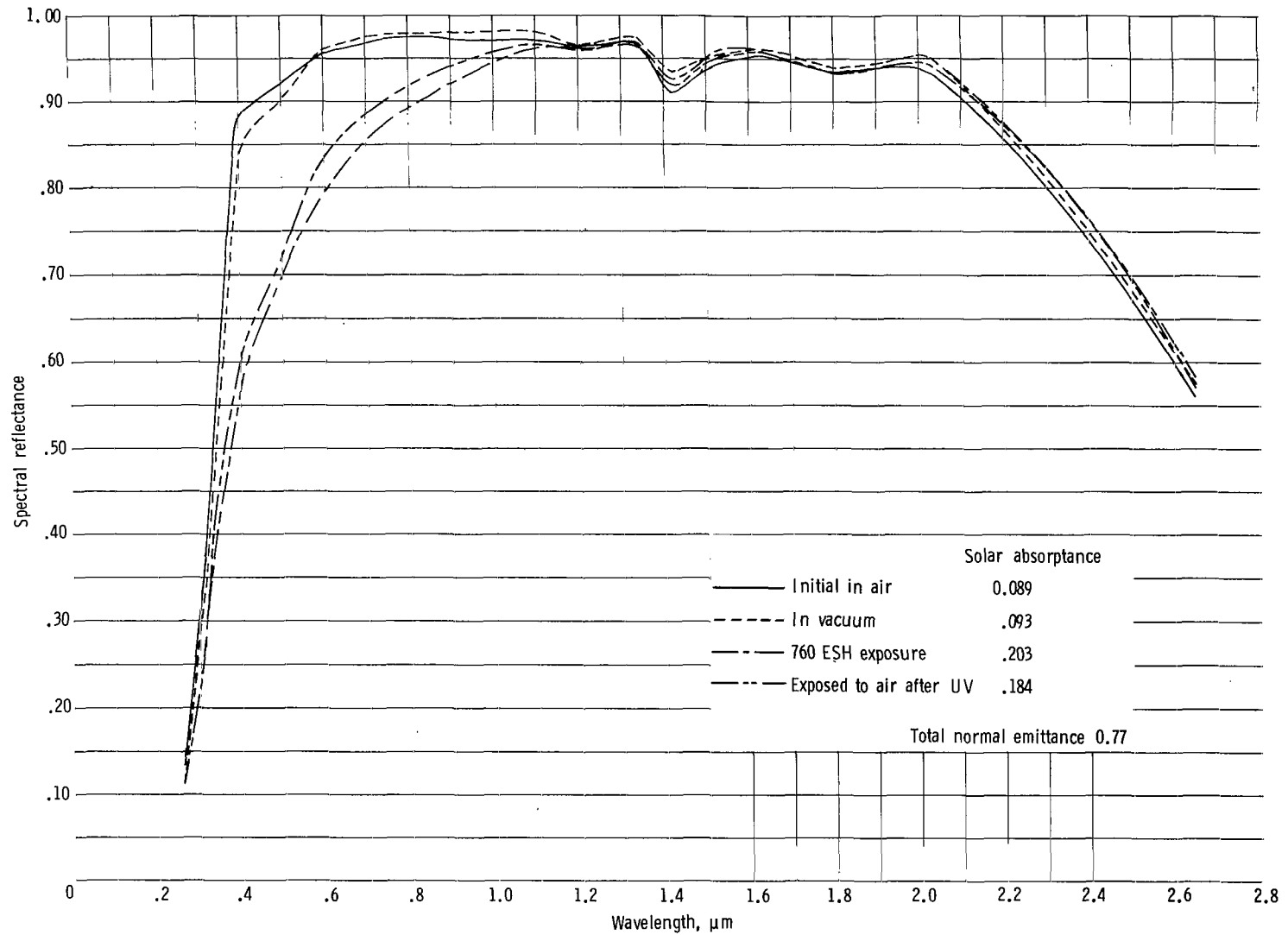
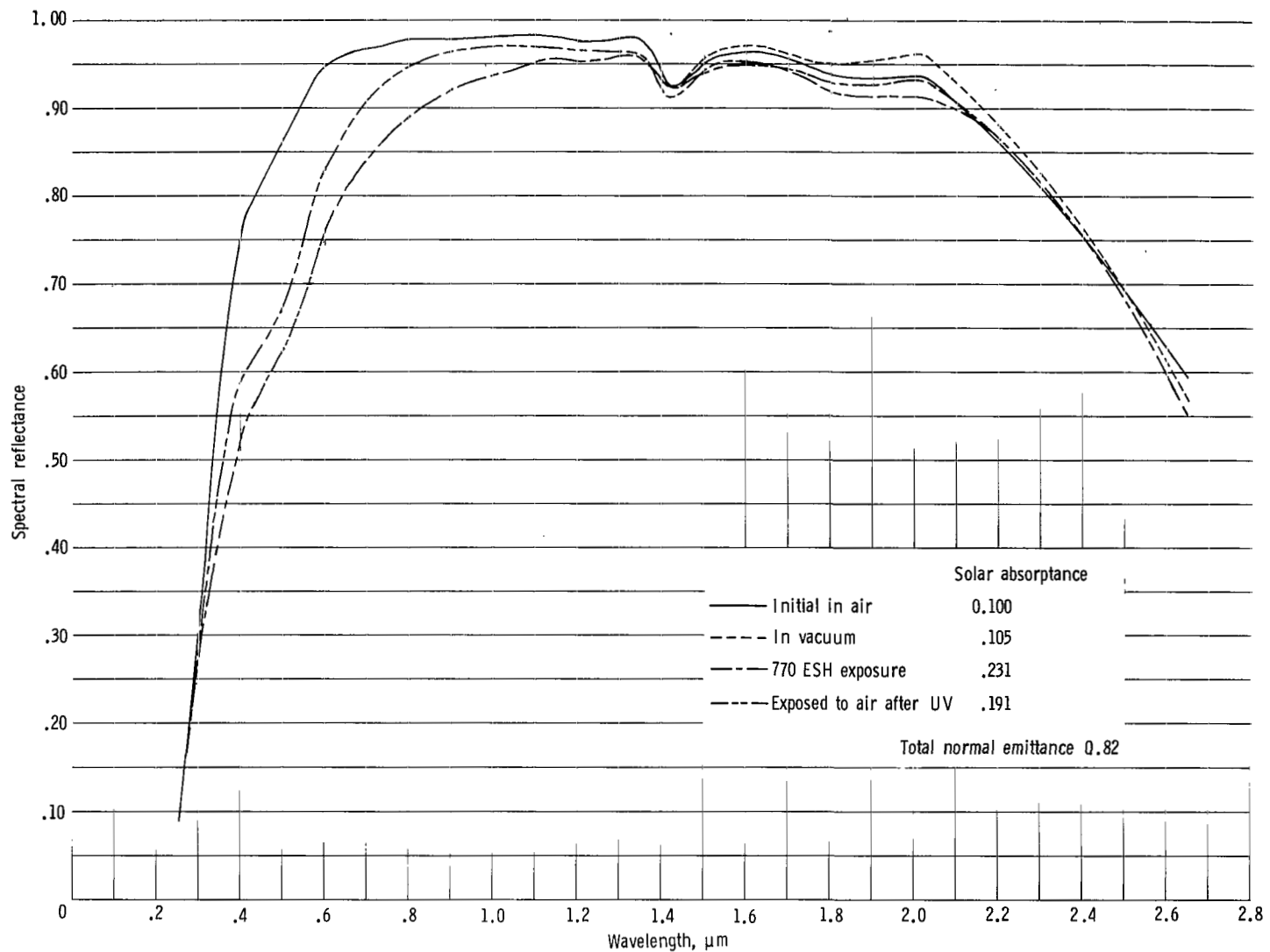
(e) $\text{Ta}_2\text{O}_5(\text{a})$ with O-I Type 650 resin.

Figure 6.- Continued.



(f) $\text{Ta}_2\text{O}_5(\text{b})$ with O-I Type 650 resin.

Figure 6.- Continued.

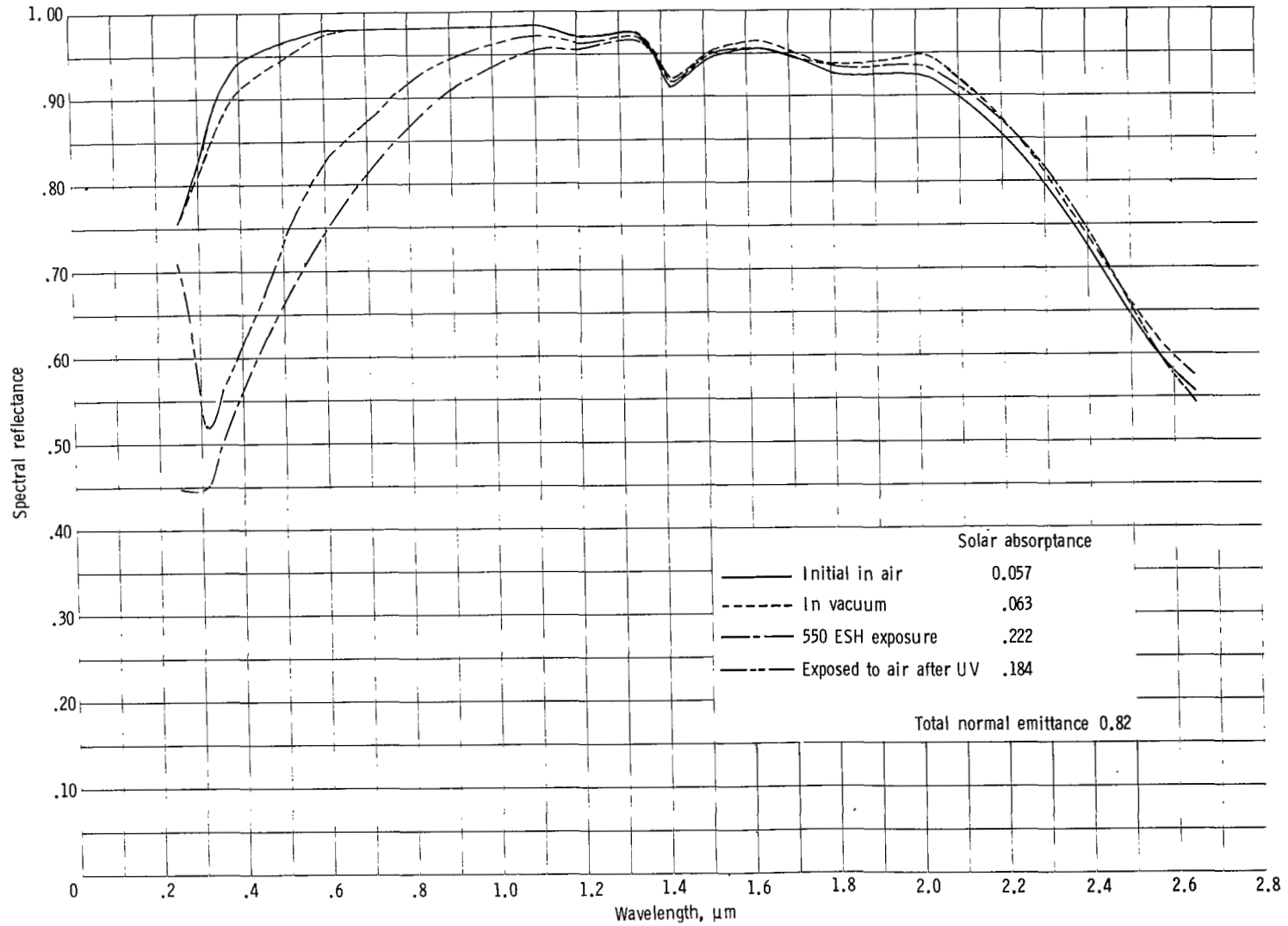
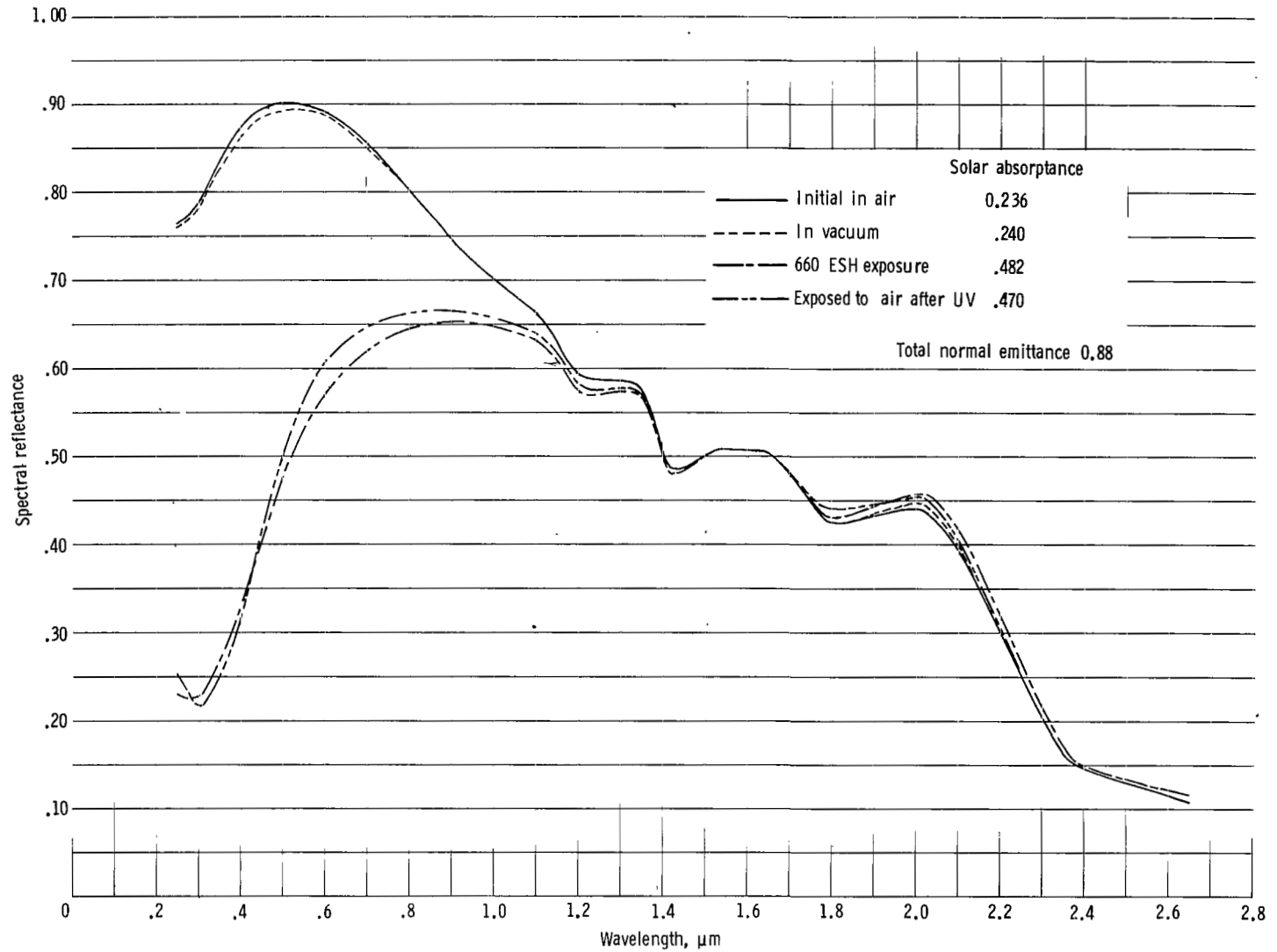
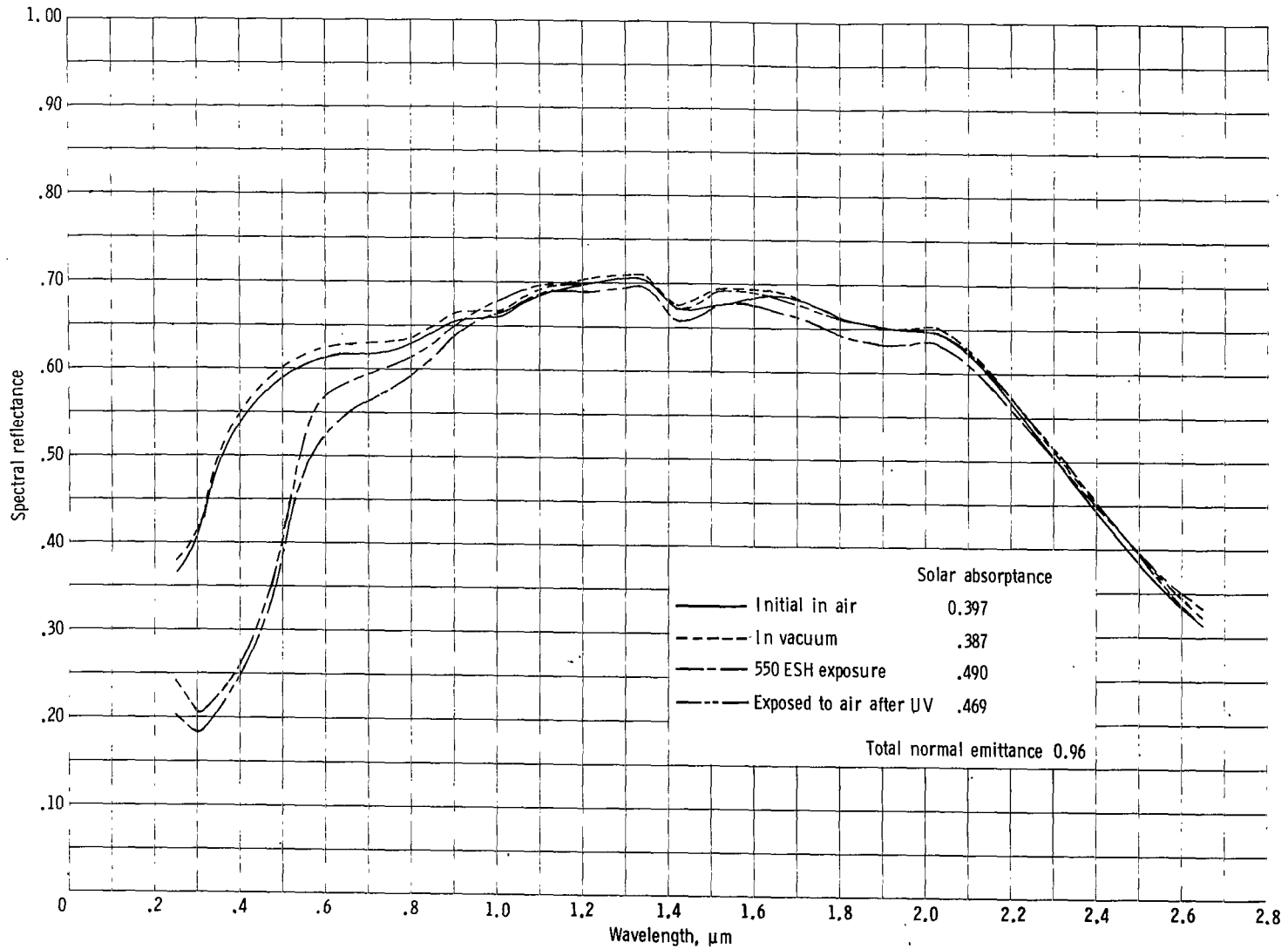
(g) $\text{ZrO}_2(\text{a})$ with O-I Type 650 resin.

Figure 6.- Continued.



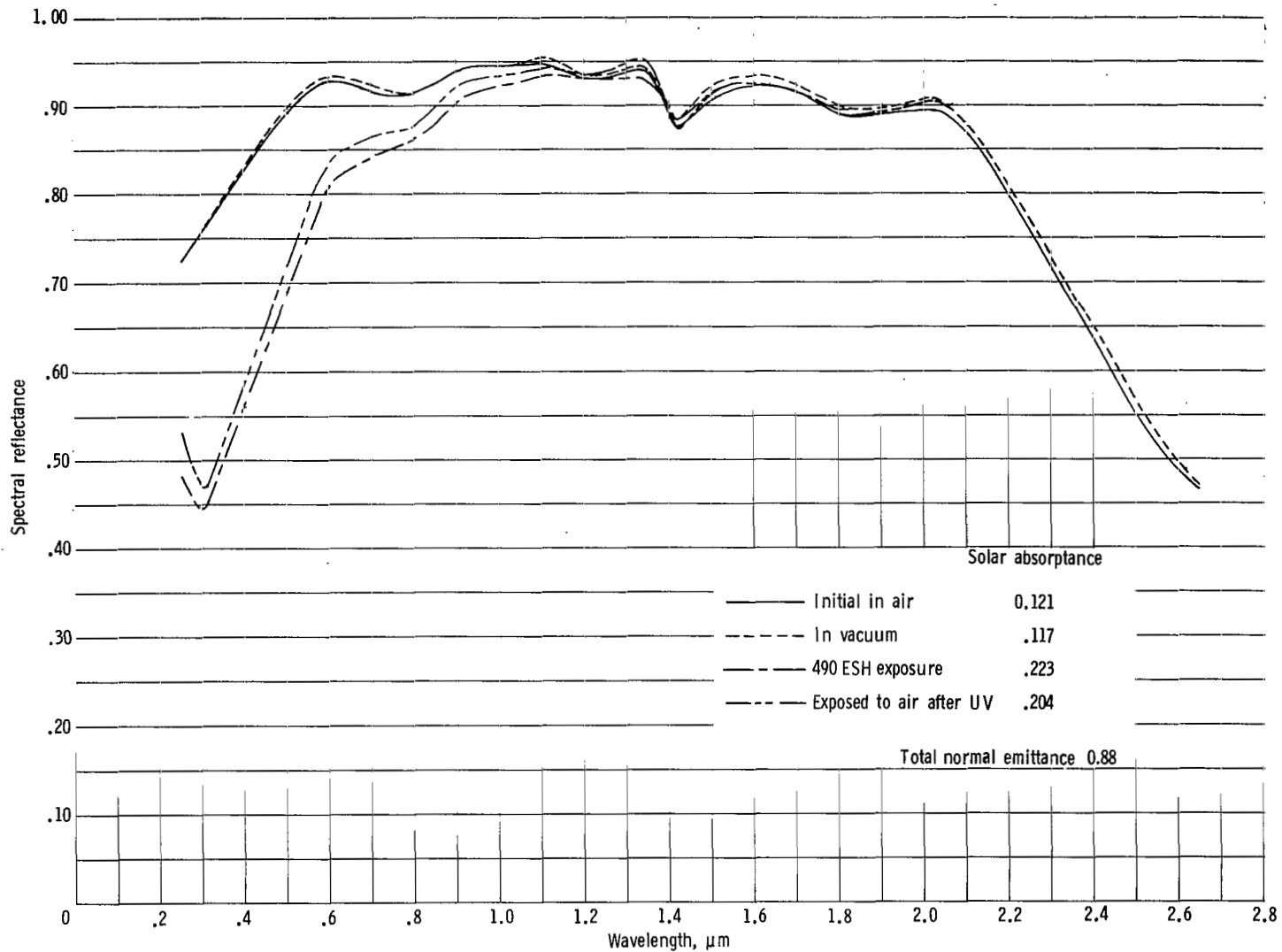
(h) $\text{ZrO}_2(\text{b})$ with O-I Type 650 resin.

Figure 6.- Continued.



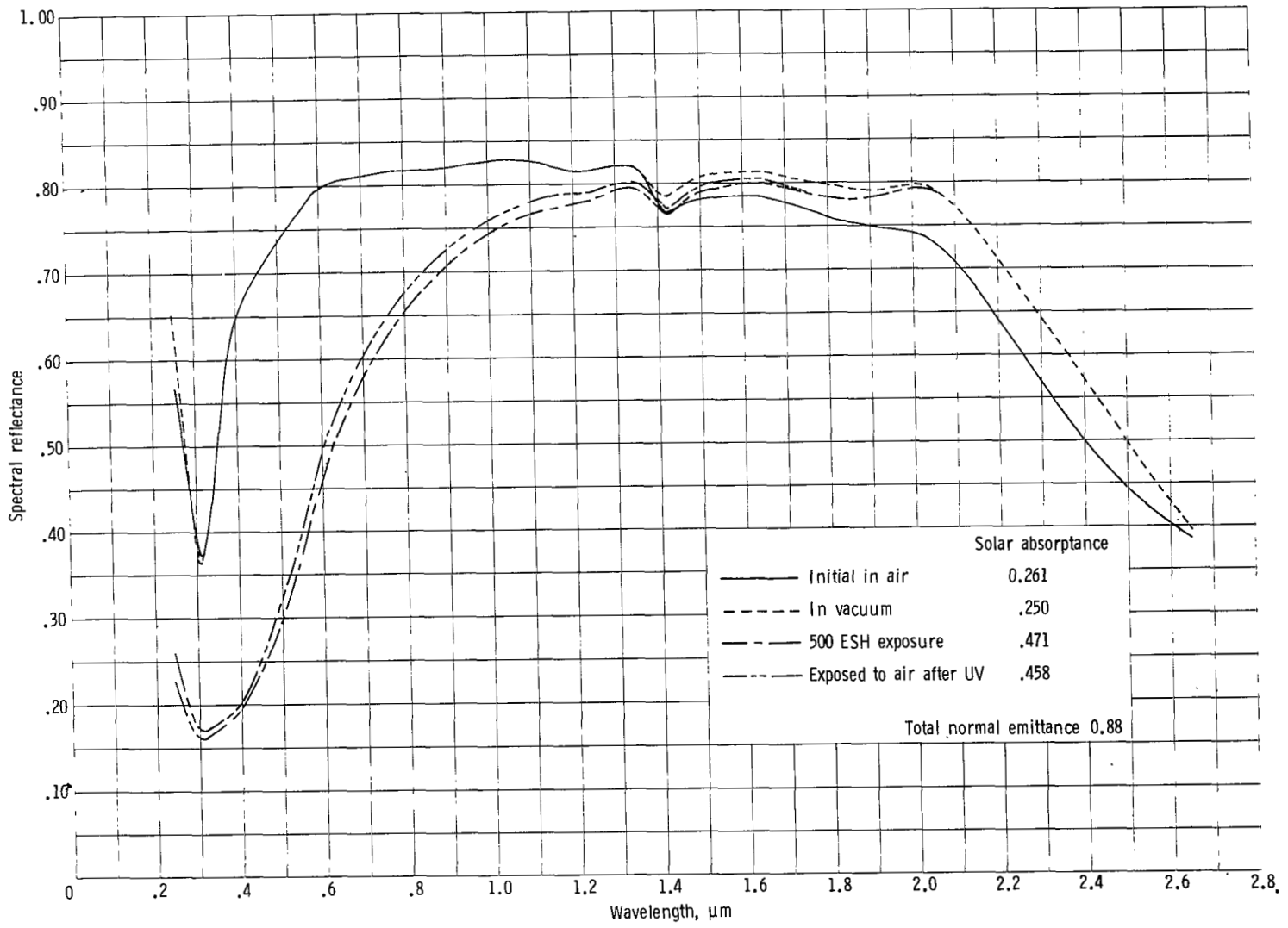
(i) BN(a) with O-I Type 650 resin.

Figure 6.- Continued.



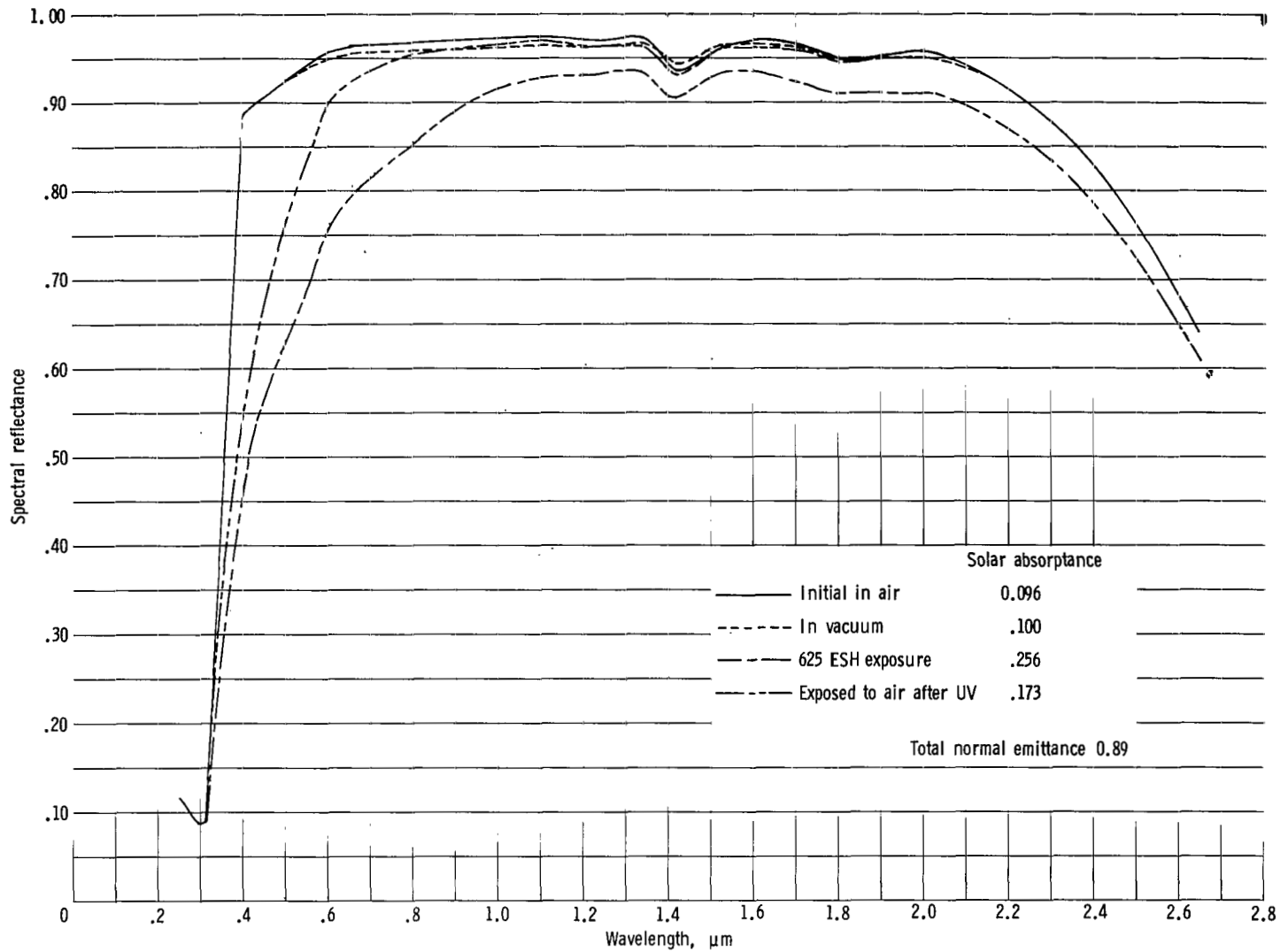
(j) BN(b) with O-I Type 650 resin.

Figure 6.- Continued.



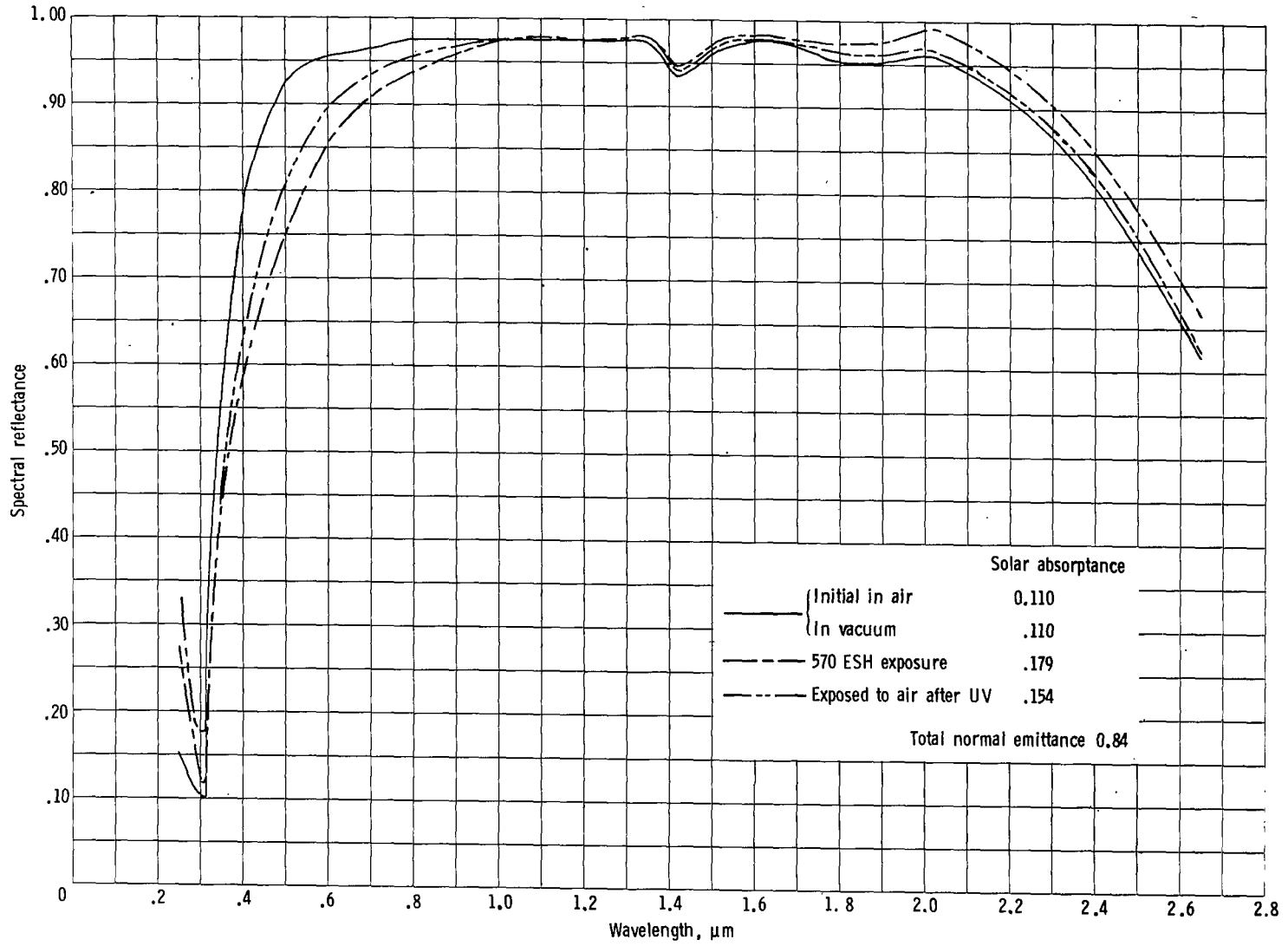
(k) BN(c) with O-I Type 650 resin.

Figure 6.- Continued.



(1) KTaO_3 with O-I Type 650 resin.

Figure 6.- Continued.



(m) ZnS with O-I Type 650 resin.

Figure 6.- Concluded.

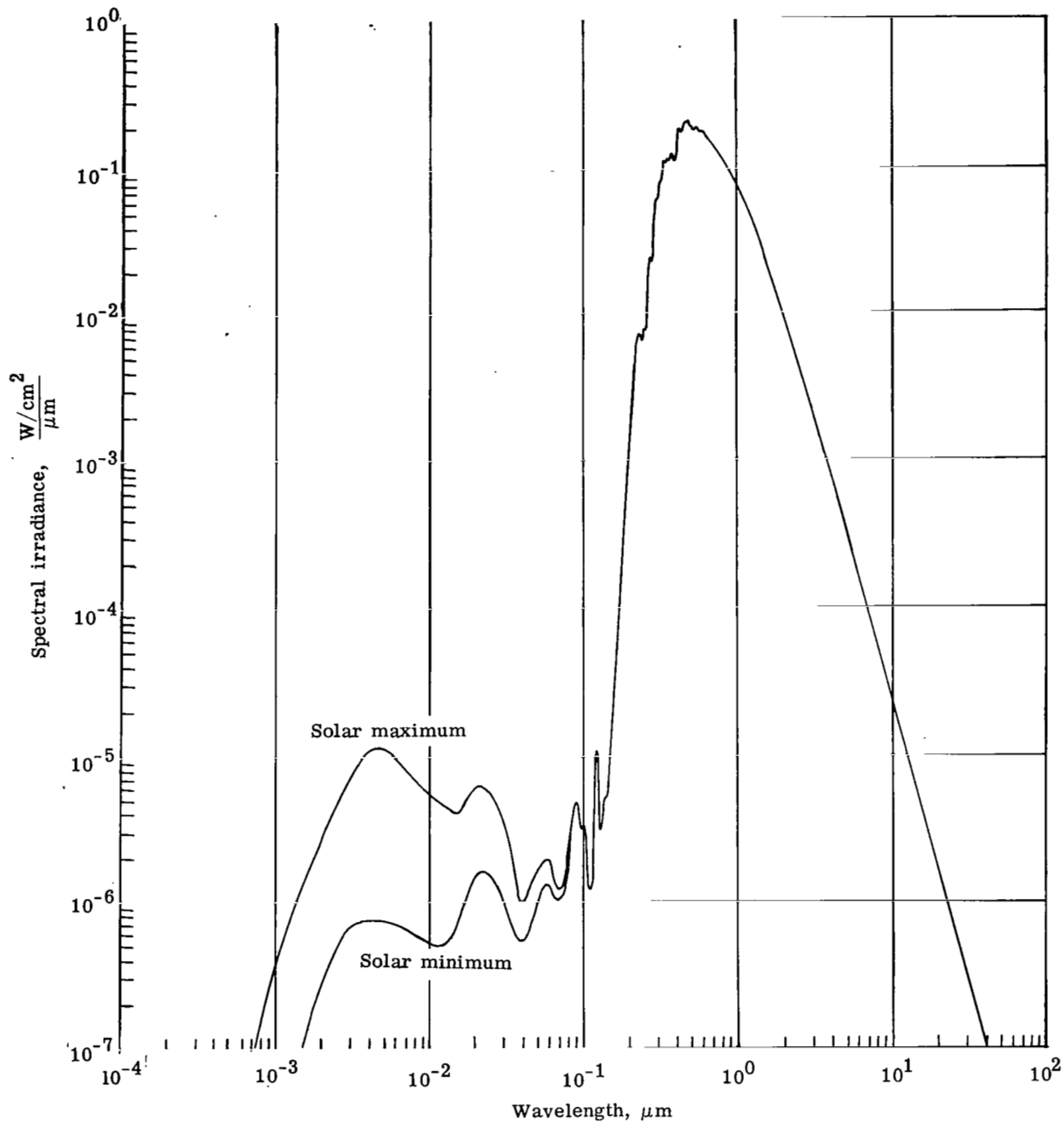


Figure 7.- The solar electromagnetic radiation spectrum (ref. 4).

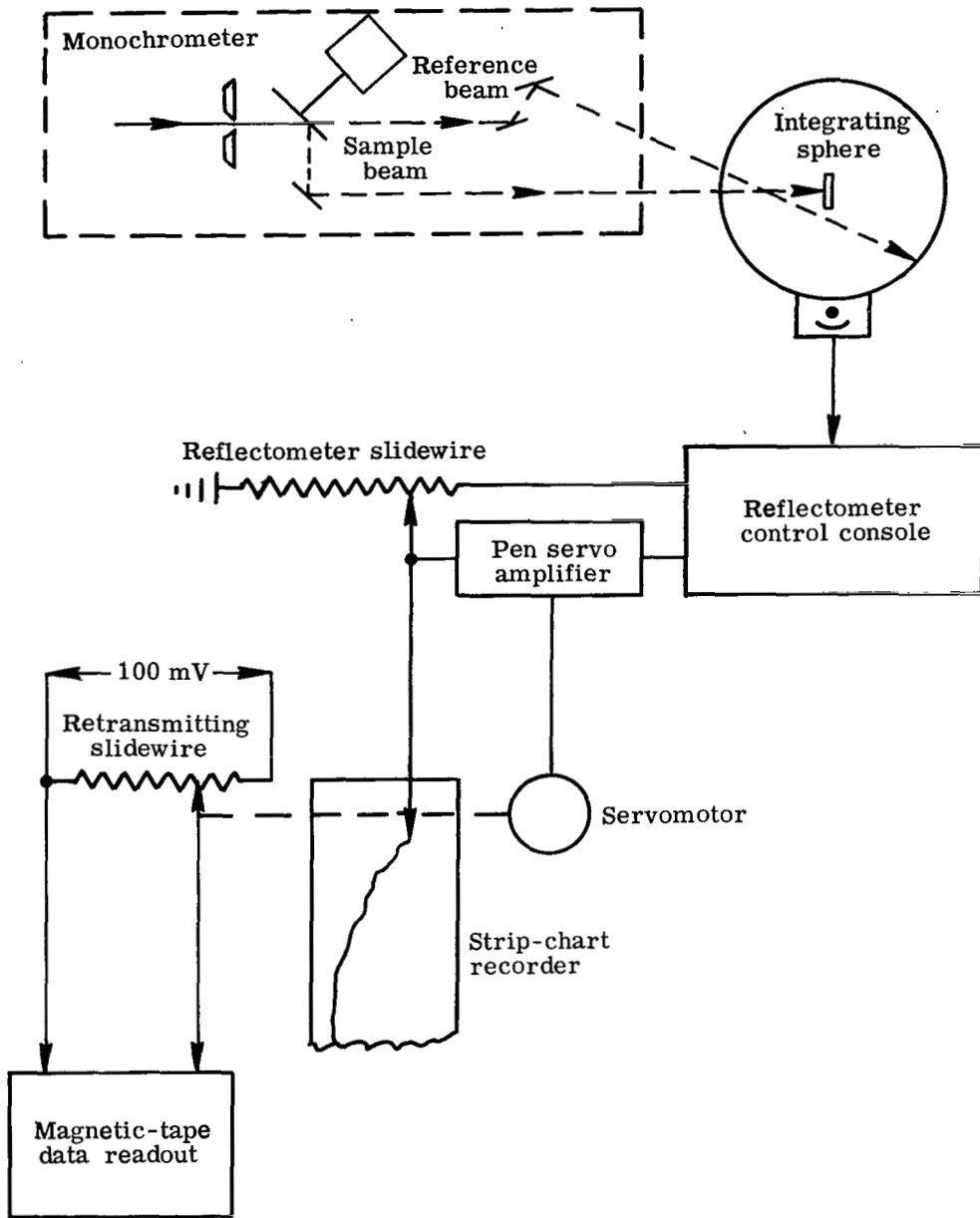


Figure 8.- Schematic diagram of reflectance-data readout system.